

**Refining the Chronostratigraphy of the Lower
Nanaimo Group, Vancouver Island, Canada, using
Detrital Zircon Geochronology**

**by
Chuqiao Huang**

B.Sc. (Hons.), McMaster University, 2015

Thesis Submitted in Partial Fulfillment of the
Requirements for the Degree of
Master of Science

in the
Department of Earth Sciences
Faculty of Science

© Chuqiao Huang 2018
SIMON FRASER UNIVERSITY
Fall 2018

Copyright in this work rests with the author. Please ensure that any reproduction or re-use is done in accordance with the relevant national copyright legislation.

Approval

Name: Chuqiao Huang

Degree: Master of Science (Earth Sciences)

Title: *Refining the chronostratigraphy of the lower Nanaimo Group, Vancouver Island, Canada, using detrital zircon geochronology*

Examining Committee:

Chair: Dr. Andy Calvert
Graduate Program Chair

Shahin E. Dashtgard
Senior Supervisor
Professor

H. Daniel Gibson
Supervisor
Professor

James MacEachern
External Examiner
Professor
Department of Earth Sciences
Simon Fraser University

Date Defended/Approved: December 17th, 2018

Abstract

Convergent-margin basins (CMBs) are rich in broadly coeval detrital zircon (DZ) owing to the proximity of active magmatic belts. Consequently, DZ geochronology can be employed to assess the utility of stratigraphic frameworks developed for these basins. This study uses DZ data to assess the utility of lithostratigraphy developed for the Cretaceous-aged lower Nanaimo Group in the Georgia Basin, Canada. Results show that the basal lithostratigraphic unit of the Nanaimo Group, the Comox Formation, comprises strata that are neither time correlative nor genetically related. The three lithostratigraphic units directly overlying the Comox Formation (Haslam, Extension, and Protection formations) comprise strata with similar genetic affinities, indicating that deposition of these units was not entirely sequential, and contemporaneous in some locales. Further, sediment provenance evolved through time, which the existing lithostratigraphic framework does not reflect. This work demonstrates that DZ geochronology can effectively test the utility of stratigraphic frameworks in CMBs.

Keywords: Detrital zircon geochronology; forearc basin; Insular Belt; Wrangellia

Table of Contents

| | |
|---|-----------|
| Approval..... | ii |
| Abstract..... | iii |
| Table of Contents..... | iv |
| List of Tables..... | vi |
| List of Figures..... | vii |
| List of Acronyms..... | x |
| Chapter 1. Introduction..... | 1 |
| 1.1. Thesis layout..... | 1 |
| 1.2. Introduction and research objectives..... | 1 |
| 1.3. Geological background..... | 3 |
| 1.4. Lithostratigraphy of the Nanaimo Group..... | 4 |
| 1.5. Ages derived from biostratigraphy and historical detrital zircon MDAs..... | 8 |
| 1.6. Methodology..... | 11 |
| Chapter 2. Detrital zircon results and source areas..... | 15 |
| 2.1. Maximum depositional ages..... | 19 |
| 2.2. Multi-dimensional scaling groups..... | 19 |
| 2.2.1. Group 1..... | 19 |
| 2.2.2. Group 2..... | 19 |
| 2.2.3. Group 3..... | 20 |
| 2.2.4. Group 4..... | 20 |
| 2.3. Source area interpretations..... | 20 |
| 2.3.1. Coast plutonic complex..... | 20 |
| 2.3.2. Insular Belt sources..... | 23 |
| Bonanza Arc..... | 23 |
| Sicker Group..... | 24 |
| Descon Arc..... | 24 |
| 2.3.3. Other sources..... | 24 |
| 2.4. Considerations for detrital zircon interpretations..... | 25 |
| 2.4.1. Paleoenvironment..... | 26 |
| 2.4.2. Magmatic quiescence..... | 27 |
| 2.4.3. Paleogeography..... | 28 |
| 2.4.4. Sedimentation rate..... | 29 |
| 2.4.5. Sample reliability..... | 29 |
| Chapter 3. Revisions to the history of the Georgia Basin..... | 30 |
| 3.1. A revised chronostratigraphy for the lower Nanaimo Group..... | 30 |
| 3.2. Implications for evolution of the Georgia Basin..... | 35 |
| Chapter 4. Conclusions..... | 37 |
| 4.1. Future work..... | 39 |

| | |
|---|-----------|
| References..... | 41 |
| Appendix A. Detrital zircon SEM images..... | 51 |
| Appendix B. Detrital zircon mount images..... | 52 |
| Appendix C. Detrital zircon supplementary data | 53 |
| Appendix D. DZ sample positions in core and outcrop..... | 54 |

List of Tables

| | |
|---|----|
| Table 3.1 Summary of source area changes between MDS Groups; samples 16 and 19 have been excluded as they do not reasonably portray the range of igneous/metamorphic source areas active during the deposition of their host strata. | 30 |
|---|----|

List of Figures

| | |
|--|----|
| Figure 1.1 - Evolution of Nanaimo Group lithostratigraphic nomenclature. Nomenclature has been divided into pre- and post-1970, when depositional model interpretations evolved from primarily braided river and paralic deposition to turbidite fan and levee complexes (modified from Mustard (1994)). | 2 |
| Figure 1.2 - Extent of the Nanaimo Group on land (green). The Georgia Basin is separated into the Comox and Nanaimo sub-basins by the Nanoose Uplift. | 4 |
| Figure 1.3 - Two-dimensional reconstructions of the Nanaimo Group. (A) Schematic cross-section showing the architecture of the Nanaimo Group across the Comox and Nanaimo sub-basins and utilizing the two sub-basin, 11-unit lithostratigraphic scheme (Bickford and Keynon, 1988). (B) Geological map of Vancouver Island and Hornby and Denman Islands utilizing a two-basin, 7-unit lithostratigraphic scheme (England 1989). | 7 |
| Figure 1.4 - Foraminiferal biostratigraphy (Sliter 1973; McGugan 1982), ammonite and inocerami biostratigraphy (Muller and Jeletzky 1970; Ward 1978; Haggart et al. 2005), zircon-based ages (Keynon et al. 1992), and DZ MDAs derived from Matthews et al. (2017) for the Nanaimo Group. U=upper, M=middle, L=lower. In the Dominant Lithology column, gray indicates mudstone/shale, yellow indicates sandstone and conglomerate, and black indicates coal. Rightward deflection of the Dominant Lithology reflects increasing grain size. In the Zircon age and DZ MDAs column, the hexagon is an <i>in situ</i> zircon age, and circles indicate DZ MDAs. Different colours of these shapes indicate the lithostratigraphic formation of origin for a zircon/DZ sample: Red = Comox Fm, Green = Extension Fm, Purple = Protection Fm, Grey = upper Nanaimo Group. Figure modified after Mustard (1994), England (1989) and Hamblin (2012). | 9 |
| Figure 1.5 Previous published DZ data. For each sample, information is provided on lithostratigraphic formation of origin and grain count. For example, a DZ sample taken from the Comox Fm with 248 ages is recorded as (Co; n=248). Acronyms: Co = Comox Fm, Ex = Extension Fm, Pr = Protection Fm, CD = Cedar District Fm, DC = De Courcy, No = Northumberland Fm, Ge = Geoffrey, Sp = Spray, Ga = Gabriola. Samples are colour-coded by study. | 11 |
| Figure 1.6 Sample sites for DZ samples published in this study. Colours indicate the lithostratigraphic unit from which a sample was taken. The line of section is depicted in Figure 3.2. | 12 |
| Figure 2.1 Normalized detrital zircon U-Pb spectra displayed as KDEs (filled) and PDPs (lines). Significant age modes (grains in that mode represent >3% of the sample) are labelled. Below the sample name are the lithostratigraphic formation. The “n” values at the far right are the number of concordant grains measured in each sample; below are interpreted depositional environment (Appendices C and D) and MDS group (Fig. 2.3). Y-axis is normalized probability. Kernel-density estimation plots are colour coded by formation using the same colour code as Figure 1.6. Red = Comox Fm, Blue = Haslam Fm, Green = Extension Fm, and Purple = Protection Fm. | 17 |

- Figure 2.2 Plot of MDAs derived from samples. Sample number is shown on the x-axis and MDA on the y-axis. Coloured circles represent the MDA, and vertical lines show the uncertainty in ages. Maximum depositional ages are based on Y3G @ 2σ . The grey and white bands behind the samples shows the age range of the Geologic Age intervals (gray letters). Samples are colour coded by formation using the same colour code as Figure 1.6. Red = Comox Fm, Blue = Haslam Fm, Green = Extension Fm, and Purple = Protection Fm..... 17
- Figure 2.3 Two-sample non-metric Kolmogorov-Smirnov statistic MDS plot assessing similarities of DZ samples 1–21. Four MDS groups are defined based on nearest-neighbour analysis. Barring Group 4, DZ samples sharing a group have nearest neighbours which map to another member of the group. Artificial populations at 360, 200, 170, 150, 120 and 93 Ma are also provided; these ages represent the most prevalent modes in the DZ samples. A stress value of 0.089041 indicates that the 2-dimensional distances between samples displayed on the plot are a fair approximation of the multi-dimensional differences between samples (Kruskal 1964). Samples are colour coded by formation using the same colour code as Figure 1.6. Red = Comox Fm, Blue = Haslam Fm, Green = Extension Fm, and Purple = Protection Fm..... 18
- Figure 2.4 Dates of 190–70 Ma plutons from the northern ($>52^\circ$ N) and southern (49 to 51° N) CPC, and their magmatic fluxes over time. Distance in northern CPC is relative to the Coast shear zone, and distance in the southern CPC is relative to the Nanaimo Group. Each dot represents a single zircon or titanite age, and the filled grey curves are KDEs of plutons. Figure modified after Gehrels et al. (2009) and Matthews et al. (2017). Data for northern CPC is compiled from Gehrels et al. (2009) and data for the southern CPC is compiled from Friedman and Armstrong (1995).....22
- Figure 2.5 Modern outcrops of interpreted source areas. Modified from Wheeler and McFeely (1991).25
- Figure 3.1 Interpreted sequence stratigraphy of the lower Nanaimo Group in the Comox Sub-Basin based on facies analysis, stratigraphic correlation and DZ MDAs (modified after Kent et al. (in review)). Strata are grouped into four depositional systems: braided-fluvial, coastal plain, paralic & shallow-marine, and marine. The position of DZ samples taken from the Comox Sub-Basin are shown on the vertical sections (vertical black lines). Acronyms: Formation = Fm; Member = Mbr.33
- Figure 3.2 (A) Interpreted chronostratigraphy of the lower Nanaimo Group shown as a Wheeler Diagram for the Georgia Basin, based on DZ. Orange units are conglomerate dominated, green units are mudstone dominated, yellow units are sandstone dominated, and gray units are shale and mudstone dominated. The white area below the red line at the base of the Nanaimo Group represents both non-deposition and pre-Nanaimo Group strata (e.g., Jurassic volcanics) while the gray-hashed areas represent non-deposition / erosion within the Nanaimo Group. Circles and numbers indicate MDAs derived from DZ samples and sample numbers are given. The boundary between the lower and upper Nanaimo Groups is placed in the Campanian to reflect results from biostratigraphy (Ward 1978; Haggart et al. 2005). (B) Presently accepted chronostratigraphy of the

Nanaimo Group (Ward 1978; Mustard 1994; Haggart et al. 2005). (C)
Proposed chronostratigraphy for the lower Nanaimo Group in two sub-
basins of the Georgia Basin, based on DZ geochronology. The colour of
proposed stratigraphic units correlates to the dominant lithology. (A), (B)
and (C) share the same time scale.....35

List of Acronyms

| | |
|------------------------------------|---|
| BSE | Backscattered electron |
| CA-TIMS | Chemical abrasion-thermal ionization-mass spectrometry |
| CL | Cathodoluminescence |
| CMB | Convergent margin basin |
| CPATT | Center for Pure and Applied Tectonics and Thermochronology |
| CPC | Coast plutonic complex |
| DZ | Detrital zircon |
| Fm | Formation |
| IPC | Island plutonic complex |
| KDE | Kernel density estimate |
| LA-ICP-MS | Laser ablation-inductively coupled plasma-mass spectrometry |
| Ma | Million years |
| Mbr | Member |
| MDA | Maximum depositional age |
| MDS | Multi-dimensional scaling/scaled |
| S | Sample |
| SEM | Scanning electron microscopy |
| SFU | Simon Fraser University |
| WCC | West coast crystalline complex |
| Y3G @ 2σ | Youngest three grain cluster overlapping at two sigma uncertainty |
| Y3G+ @ 2σ | Youngest three or more grain cluster overlapping at two sigma uncertainty |
| YSG | Youngest single grain |

Chapter 1. Introduction

1.1. Thesis layout

This thesis is divided into four chapters. Chapter one introduces the study, research objectives, and methodology, and provides a summary of previously published works on lithostratigraphy, biostratigraphy, and DZ geochronology in the Nanaimo Group. Chapter two summarizes the data collected in this study, discusses limitations of the dataset and proposes potential source areas. Chapter three uses data from chapter two to refine the chronostratigraphy of the lower Nanaimo Group, and infer tectonic evolution of the Insular Belt. Finally, Chapter four summarizes the main results with respect to the research objectives.

1.2. Introduction and research objectives

Lithostratigraphy organizes strata based on lithology, but due to its limited use in resolving time-equivalency of strata and basin evolution, lithostratigraphy has largely been succeeded by genetic stratigraphy. Despite this, the strata of many convergent-margin basins (CMBs), including forearc basins such as the Georgia Basin, Canada, are characterized by lithostratigraphic frameworks that generate constructs which are often mistakenly interpreted to record sequential, vertical filling of the basin (Fig. 1.1; e.g. McCarron 1997; Takashima et al. 2004; Aksoy et al. 2005). Convergent-margin basins form in response to the subduction of oceanic lithosphere, and are situated in close proximity to active magmatic belts. Consequently, the fill of CMBs is typically rich in broadly coeval detrital zircon (DZ), and maximum depositional ages (MDAs) generated from DZ datasets can be analyzed to constrain depositional ages and sediment provenance (Dickinson and Gehrels 2009; Cawood et al. 2012; Englert et al. 2018). A sequentially filled CMB should be manifested as progressively younger DZ MDAs, as MDAs have been shown to closely approximate true depositional age in CMBs.

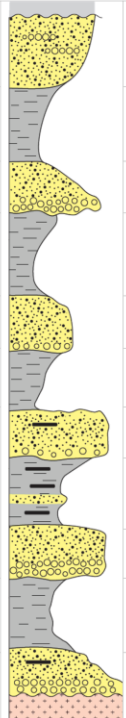
| Pre-1970 nomenclature | | | | Post-1970 nomenclature | | | | | | | |
|---|----------------------------|--|-----------------|-------------------------------|---------------------|----------------------------|-------------------|--------------------------------|--|-------------------|--|
| Early Studies – Evolving Nomenclature | | | | Two Basins, Two Nomenclatures | | | | One Basin, One Nomenclature | | | |
| Nanaimo Basin | | Comox Basin | | Nanaimo Basin | | Comox Basin | | Nanaimo Basin | | | |
| Clapp (1914), Buckham (1947), Usher (1952) | Clapp & Cooke (1917) | Williams (1924), Mackenzie (1922) | Usher (1952) | England (1989) | McGugan (1990) | England (1989) | McGugan (1990) | Muller & Jeletzky (1970) |  | | Ward (1978), Mustard (1994), and later |
| Gabriola | Gabriola | St. John | Hornby | Gabriola | Gabriola | Hornby | Hornby | Gabriola | Gabriola | Gabriola | |
| North- umberland | North- umberland | Cowichan Basin | Tribune | Spray | Mayne | North- umberland | Spray | Spray | Spray | Spray | |
| | | | Hornby | Geoffrey | Galiano | | Geoffrey | Geoffrey | Geoffrey | Geoffrey | |
| | | | Lambert | Lambert | North- umberland | Lambert | Upper Lambert | North- umberland | North- umberland | | |
| | | | De Courcy | De Courcy | De Courcy | De Courcy | Denman | Lower Lambert | De Courcy | De Courcy | |
| Cedar District | Cedar District | | Duncan | Trent River | Trent River | Cedar District | Cedar District | Trent River | Upper Trent River | Cedar District | Cedar District |
| Protection | Protection | Protection | | | | Protection | Protection | | | | |
| Newcastle | Ganges | Trent River | Trent River | Trent River | Pender | Newcastle | Trent River | Upper Trent River | Extension- Protection | Pender | |
| Cranberry | | | | | Cranberry | | | | | | |
| Extension | Extension | Extension | Trent River | Trent River | Extension | Extension E. Willington | Trent River | Lower Trent River | Haslam | Extension | |
| E. Willington | | | | | Haslam | Haslam | | | | Haslam | Haslam |
| Haslam | Haslam | Comox | Comox | Comox | Haslam | Haslam | Comox | Dunsmuir Benson | Comox | Haslam | |
| Benson | Benson | | | | Benson | Benson | | | | Comox | Comox |

Figure 1.1 - Evolution of Nanaimo Group lithostratigraphic nomenclature. Nomenclature has been divided into pre- and post-1970, when depositional model interpretations evolved from primarily braided river and paralic deposition to turbidite fan and levee complexes (modified from Mustard (1994)).

In this study, I evaluate the degree of diachroneity encompassed by lithostratigraphic units within the lower Nanaimo Group, Georgia Basin, Canada using DZ geochronology. I use MDAs to define chronostratigraphic boundaries, and propose revisions to the presently accepted depositional history of the Nanaimo Group. I also use multi-dimensional scaling (MDS) to assess changes in sediment provenance within and between currently employed lithostratigraphic units. From these data, I reconstruct, in part, the depositional history of the Georgia Basin, and demonstrate that DZ geochronology can be used to evaluate stratigraphic frameworks in CMBs globally. To achieve these goals, three main objectives are defined:

1. Collect DZ samples across the breadth of the lower Nanaimo Group, with a focus on strata nearest the basal unconformity. Use DZ populations to generate age distributions, maximum depositional ages, and a multi-dimensional scaled plot.

2. Utilize DZ MDAs to assess changes in depositional age within and between lithostratigraphic formations. Employ the MDS plot and age distributions to assess changes in sediment provenance within and between lithostratigraphic formations. Use results to test the capabilities of lower Nanaimo Group lithostratigraphy in predicting litho-formation depositional age and depositional order.
3. Employ MDS of DZ populations, age distributions and MDAs to infer additional subsidence and sedimentation events in the Georgia Basin, and generate an interpreted chronostratigraphy.

1.3. Geological background

The Nanaimo Group comprises a 4 km-thick package of mainly Turonian- to Maastrichtian-aged sedimentary rock that infills the Georgia Basin, British Columbia, Canada (Mustard 1994). The western margin of the Georgia Basin overlies the Devonian to Jurassic, exotic Wrangellia Terrane, which is part of the Insular Belt. The eastern margin overlies the Coast Plutonic Complex, a Jurassic to Eocene continental volcanic arc that forms part of the Coast Belt. Deposition of the Nanaimo Group occurred primarily in a forearc setting, mainly during the Late Cretaceous (England and Bustin 1998).

Tectonics on the western margin of the North American Cordillera during the Mesozoic were primarily driven by westward movement of the North American plate (Coney 1978; Beck Jr. and Housen 2003), which caused subduction of the Farallon and Kula oceanic plates. This process transported and accreted a variety of allochthonous terranes, including Wrangellia, to the western margin of North America. Following accretion, many of these terranes were displaced northward an unknown distance relative to the North American craton (ca. 90–55 Ma). The distance of northward displacement is contentious, and is known as the “Baja BC controversy” – studies utilizing different methodologies to measure displacement yield vastly different estimations. Early paleomagnetic studies of the Nanaimo Group and surrounding Cretaceous rocks suggest a 2,500 to 3,000 km northward displacement (Beck and Noson 1972; Umhoefer 1987; Ague and Brandon 1996; Enkin et al. 2001). More recent paleomagnetic studies incorporating compaction corrections and known fault offsets suggest a more moderate 1,600 to 2,000 km of displacement (Kim and Kodama 2004; Krijgsman and Tauxe 2006; Umhoefer and Blakey 2006). Studies focusing on stratigraphic correlations between similar packages of strata and measured offsets on

known faults (Price and Carmichael 1986; Monger 1997; Wylde and Umhoefer 2006) suggest a modest < 1,000 km of offset. Finally, results from detrital zircon studies have been interpreted to suggest displacements ranging from < 500 km (Mahoney et al. 1999) to 2,500 km (Matthews et al. 2017).

The Nanaimo Group today is a remnant that is the result of extensive post-depositional deformation and erosion (Mustard 1994). The main Nanaimo Group outcrops are located across southeastern Vancouver Island, and are separated into two sub-basins by a paleotopographic high called the Nanoose Uplift (Fig. 1.2).

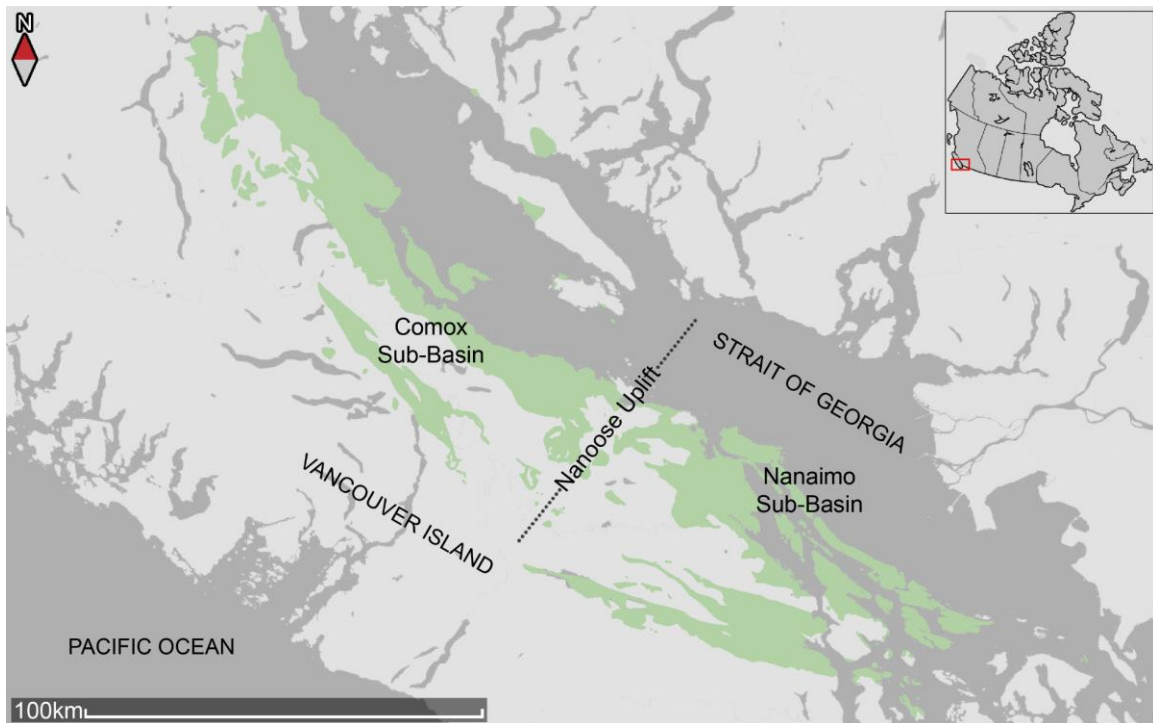


Figure 1.2 - Extent of the Nanaimo Group on land (green). The Georgia Basin is separated into the Comox and Nanaimo sub-basins by the Nanoose Uplift.

1.4. Lithostratigraphy of the Nanaimo Group

Work on the Nanaimo Group has been motivated largely by economic coal deposits in the area, which were vital to early railroads. One-hundred and fifty years of study has led to the development of a lithostratigraphic framework based on the positions of alternating, through-going, coarse clastic (sandstone and conglomerate) and finer grained (mudstone and shale) successions relative to the basal nonconformity and

to each other (Mustard, 1994). Formation ages are determined by molluscan (Muller and Jeletzky 1970; Ward 1978; Haggart et al. 2005) and microfaunal biostratigraphy (Muller and Jeletzky 1970; Ward 1978; Haggart et al. 2005).

Since the first framework was proposed by Clapp (1914), Nanaimo Group nomenclature has undergone a complex evolution (Fig. 1.1). As modern Nanaimo Group outcrops are geographically separated, early researchers (e.g., Richardson 1877; Clapp 1912) separated broadly contemporaneous strata into three sub-basins: Comox, Nanaimo and Cowichan. Clapp (1912) described the Comox and Nanaimo sub-basins as being on either side of the Nanoose Uplift, while the Cowichan Sub-Basin occurs south of the Nanaimo Sub-Basin and extends northwestward to Cowichan lake.

Following recognition that strata in the Cowichan Sub-Basin were synonymous with those in the Nanaimo Sub-Basin, Clapp (1914) revised the nomenclature down to two sub-basins (Comox and Nanaimo), and applied the formation names of the Nanaimo Sub-Basin to those in the former Cowichan Sub-Basin. However, Clapp (1911) did not extend the Nanaimo Sub-Basin formation names north into the Comox Sub-Basin, and only gave names to the two lowest formations: the basal, coal-bearing units were named the “Comox Formation”, while the overlying shales were called the “Trent River Shales”. Additions to and refinements of formation names in the Comox Sub-Basin were proposed by later authors (e.g. Williams 1924; Buckham 1947; Usher 1952).

Based on biostratigraphic ages, Muller and Jeletzky (1970) predicted that the separated outcrop areas represent the erosional remnants of a single basin and proposed a single basin model with 9 lithostratigraphic formations (Muller and Jeletzky 1970). This classification scheme was expanded later to 11 formations (Ward 1978; Mustard 1994) and has been widely accepted. The 11 formations are grouped into the lower and upper Nanaimo Group. In ascending order, the lower Nanaimo Group comprises the Comox, Haslam, Extension, Pender and Protection formations, and the upper Nanaimo Group consists of the Cedar District, De Courcy, Northumberland, Geoffrey, Spray and Gabriola formations.

A number of 2D stratigraphic architectures have been proposed, based on both the one- and two- sub-basin lithostratigraphic frameworks (Fig. 1.3). Bickford and Kenyon (1988) presented a cross section of the Nanaimo Group based on two sub-

basins, and their lithostratigraphy is modified after Usher (1952; Fig. 1.3A). The Bickford and Kenyon (1988) model depicts alternating coarse- and fine-grained units that occur in both sub-basins (Comox and Nanaimo). The surfaces between the units are highly diachronous (e.g., the top of the Dunsmuir Mbr of the Comox Fm ranges from middle Santonian to Early Campanian in age), and go through the Nanoose Uplift. England (1989) proposed an alternate view of the stratigraphy in the Comox Sub-Basin, focusing in the region around Hornby and Denman Islands (Fig. 1.3B). The alternating, coarse- and fine-grained formations in England's model are also depicted as sequentially deposited and interfingering strata with diachronous boundaries. The England (1989) model also employs the lithostratigraphic framework of Usher (1952) based on two sub-basins, and the sandstone-dominated Comox Fm is depicted as pinching out into shales of the Trent River Fm towards the southeast.

The lithostratigraphic framework was developed to map lithologies in the field, and not to resolve the temporal equivalency of strata within and between sub-basins of the Nanaimo Group. For example, the utilization of lithology rather than chronostratigraphic surfaces to subdivide the stratigraphy hinders paleoenvironmental reconstructions of the Georgia Basin during the Cretaceous. Paleoenvironments are presently interpreted through identification of sedimentological and ichnological characteristics of facies (Mustard 1994), and without consideration of spatial or temporal variations in environments. An example of this is the Extension Fm, which is encased in marine shales of the Haslam Fm below and Pender Fm above. Outside the city of Nanaimo, the Extension Fm is interpreted to represent the deposits of a submarine fan system (Ward 1978; Pacht 1984; Mustard 1994), whereas around Nanaimo it is considered to represent deltaic and braided fluvial deposits (Muller and Jeletzky 1970; Mustard 1994). While these disparate deposits appear to reside at similar stratigraphic levels, markedly different depositional scenarios are observed. Determining their actual stratigraphic relationships requires the establishment of a sequence stratigraphic framework (Bain and Hubbard 2016; Kent et al. in review), and such a framework cannot be based on the pre-existing lithostratigraphy.

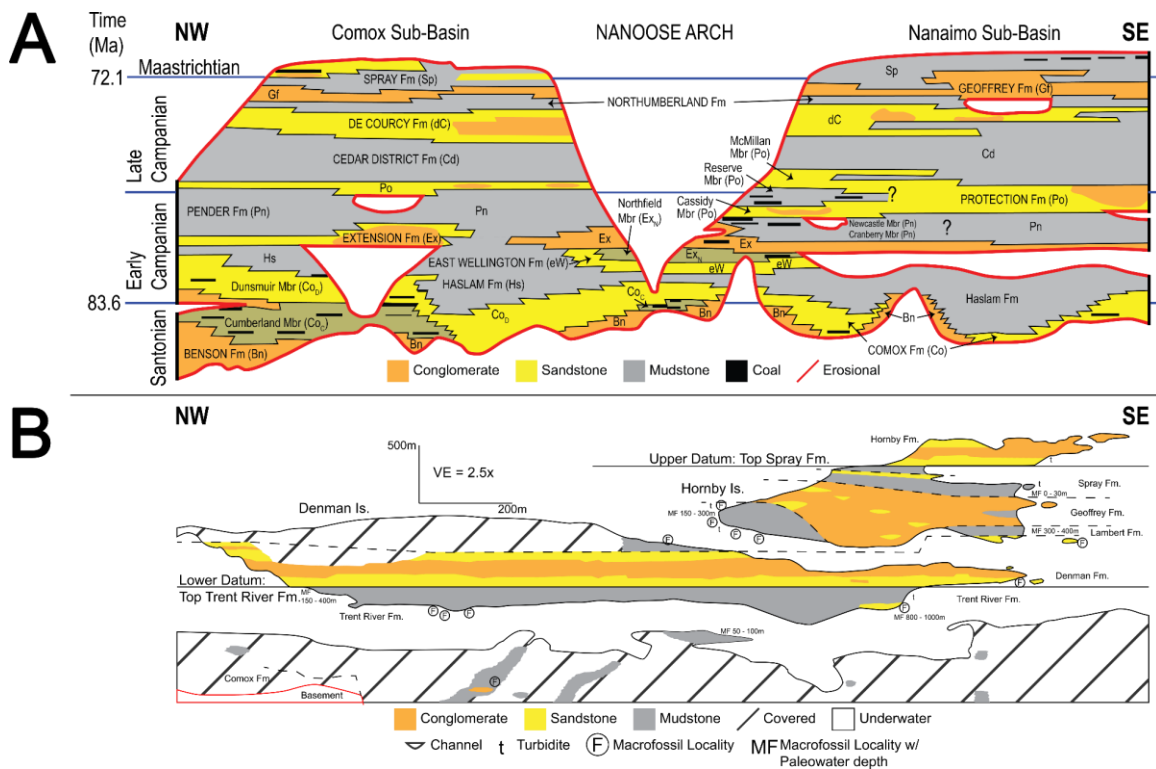


Figure 1.3 - Two-dimensional reconstructions of the Nanaimo Group. (A) Schematic cross-section showing the architecture of the Nanaimo Group across the Comox and Nanaimo sub-basins and utilizing the two sub-basin, 11-unit lithostratigraphic scheme (Bickford and Keynon, 1988). (B) Geological map of Vancouver Island and Hornby and Denman Islands utilizing a two-basin, 7-unit lithostratigraphic scheme (England 1989).

The one-basin lithostratigraphic nomenclature presently used in the Georgia Basin (Mustard 1994; Hamblin 2012) is also problematic for correlating physically stratigraphy from the Comox Sub-Basin to the Nanaimo Sub-Basin. Strata in the Comox Sub-Basin are relatively undeformed (Kent et al. in review), whereas those in the Nanaimo Sub-Basin are extensively faulted and folded by Cenozoic tectonic events (e.g. (e.g., Yorath et al. 1985; Clowes et al. 1987; England 1989; England and Calon 1991; Mustard 1994; Journeay and Morrison 1999)). This makes stratigraphic correlations difficult across and between sub-basins without timing constrained by biostratigraphy or, in rare cases, DZ MDAs. Consequently, regional correlations such as the 2D framework by Bickford and Kenyon (1988) remain untested.

1.5. Ages derived from biostratigraphy and historical detrital zircon MDAs

Molluscan biostratigraphic zonation is principally used to assign depositional ages to lithostratigraphic formations in the Nanaimo Group (Fig. 1.4). The first macrofaunal zonation scheme was proposed by Usher (1952) who defined four ammonite assemblage zones that correlate to Late Cretaceous (Santonian to Maastrichtian) stages. This was later expanded by Muller and Jeletzky (1970) to include four additional biostratigraphic subdivisions based on assemblage zones and subzones of ammonites and inocerami. Ward (1978) rearranged previously defined biostratigraphic divisions and established new ammonite zones and zonules, and Haggart et al. (2005) proposed four Turonian assemblage zones based on ammonites found in close stratigraphic proximity to the basal nonconformity in the southern-most extent of the Nanaimo Sub-Basin.

Presently, biozonation in the lower Nanaimo Group is too-coarse resolution to precisely establish chronostratigraphic relationships. Biozones overlap at the age-level, leading to uncertain differences in the implied depositional age between vertically adjacent formations. For example, the Pender Fm belongs to the *Baculites chicoensis* biozone, and the Extension Fm belongs to the *Sphenoceras ex gr. schmidti* biozone (Ward 1978). As both biozones belong to lower Campanian strata, biostratigraphy by itself cannot meaningfully distinguish between Pender and Extension formation strata.

In unfossiliferous strata, such as the majority of the Extension and Protection formations (Ward 1978), depositional ages are constrained using biozones of vertically adjacent formations or through uncertain correlations to fossil-bearing outcrops. For example, Muller and Jeletzky (1970) indicate that the shales exposed along the Trent River (SW of the Inland Island Highway) are unfossiliferous, but could be reasonably correlated to either the lower Campanian *Schmidti* zone, placing them in Haslam Fm, or the upper Campanian *Vancouverense* zone, placing them in the Cedar District Fm (cf. Fig. 1.4). Previous authors, such as Usher (1952), have been aware of conflicts between biochronology and lithostratigraphy, and have elected to subordinate the biochronology to the lithostratigraphy where contradictions arise.

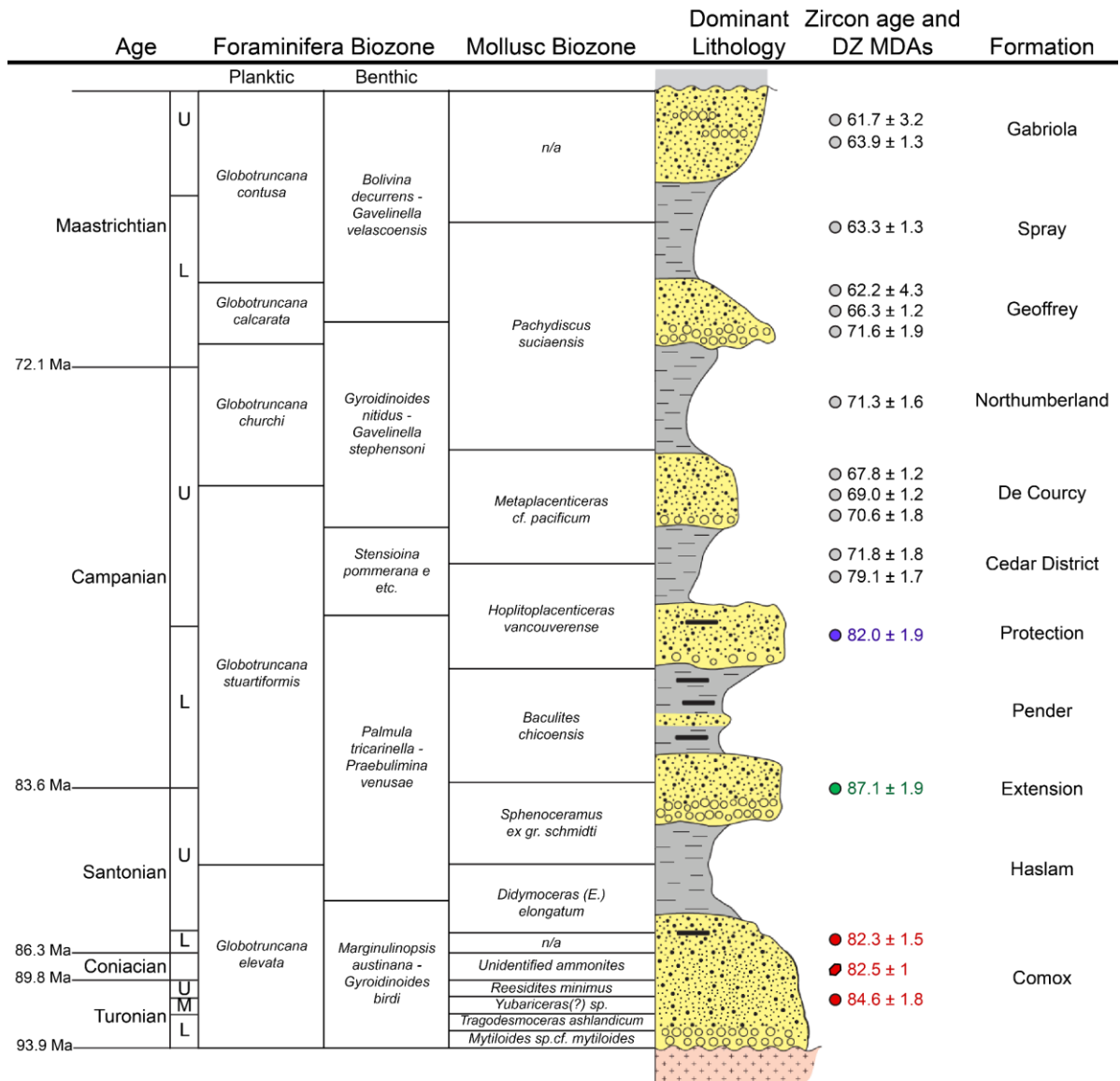


Figure 1.4 - Foraminiferal biostratigraphy (Sliter 1973; McGugan 1982), ammonite and inocerami biostratigraphy (Muller and Jeletzky 1970; Ward 1978; Haggart et al. 2005), zircon-based ages (Kenyon et al. 1992), and DZ MDAs derived from Matthews et al. (2017) for the Nanaimo Group. U=upper, M=middle, L=lower. In the Dominant Lithology column, gray indicates mudstone/shale, yellow indicates sandstone and conglomerate, and black indicates coal. Rightward deflection of the Dominant Lithology reflects increasing grain size. In the Zircon age and DZ MDAs column, the hexagon is an *in situ* zircon age, and circles indicate DZ MDAs. Different colours of these shapes indicate the lithostratigraphic formation of origin for a zircon/DZ sample: Red = Comox Fm, Green = Extension Fm, Purple = Protection Fm, Grey = upper Nanaimo Group. Figure modified after Mustard (1994), England (1989) and Hamblin (2012).

Nanaimo Group microfossil zonation is based on foraminifera, although studies have also been conducted on palynomorphs. The first zonation scheme was proposed by McGugan (1962), who proposed three foraminifera zones. The scheme was heavily modified by Sliter (1973), who proposed a 9-zone scheme that distinguished between planktic and benthic foraminifera. Final modifications were made by McGugan (1979), giving rise to the 10-biozone scheme shown in Figure 1.4. While further foraminiferal studies have been published (e.g. McGugan 1990), these were not incorporated into any biozonation schemes. The use of foraminiferal biozonation to determine lithostratigraphic formation age is also problematic for establishing precise chronostratigraphic relationships. As Nanaimo Group foraminifera are solely collected from marine facies, terrestrial strata attributed to the Comox Fm are unrepresented. Many foraminiferal biozones also span multiple ages, leading to broad depositional age and uncertain lithostratigraphic formation assignments. For example, discovery of foraminifera belonging to the planktic *Globotruncana stuartiformis* biozone implies that host strata are between upper Santonian to upper Campanian in stage (Fig. 1.4), and belong to either the Haslam, Extension, Pender, Protection, Cedar District, or De Courcy formations. A higher resolution technique such as generating DZ MDAs are required to resolve more subtle differences in stage.

In addition to biostratigraphy, zircon and DZ MDA data have been acquired from the Nanaimo Group (Fig. 1.4). The only *in situ* radiometric date from the Nanaimo Group originates from a tonstein along the Iron River (northern-most extent of the Comox Sub-Basin) that is assigned to the Comox Fm (Dunsmuir Mbr) and yields a U-Pb age of 82.5 ± 1 Ma (Kenyon et al. 1992). Meanwhile, the majority of DZ analyses (Fig. 1.5) acquired prior to 2015 used low-n (<117) samples (i.e., Mustard et al. 1995; Mahoney et al. 1999) limiting the robustness of MDAs to approximate depositional age (Vermeesch 2004; Dickinson and Gehrels 2009). Matthews et al. (2017) recently published high-n DZ datasets spanning the stratigraphic height of the Nanaimo Group around Hornby and Denman Islands (Figs. 1.4 and 1.5), although the vertical position of these samples relative to the basal nonconformity is unknown. Detrital zircon samples from the lower Nanaimo Group yield youngest three grain cluster overlapping at 2σ uncertainty (Y3G @ 2σ) MDAs of 82.3 ± 1.5 Ma and 84.6 ± 1.8 Ma for the Comox Fm, 87.1 ± 1.9 Ma for the Extension Fm and 82.0 ± 1.9 Ma for the Protection Fm (Fig. 1.4). Notably, one of the Comox Fm samples yielded a Campanian MDA and the Extension Fm sample yielded a

Coniacian MDA; both fall outside the expected formation stage determined by biostratigraphy. Englert et al. (2018) published additional high-n DZ datasets (Figs. 1.4 and 1.5), although these were solely from the upper Nanaimo Group.

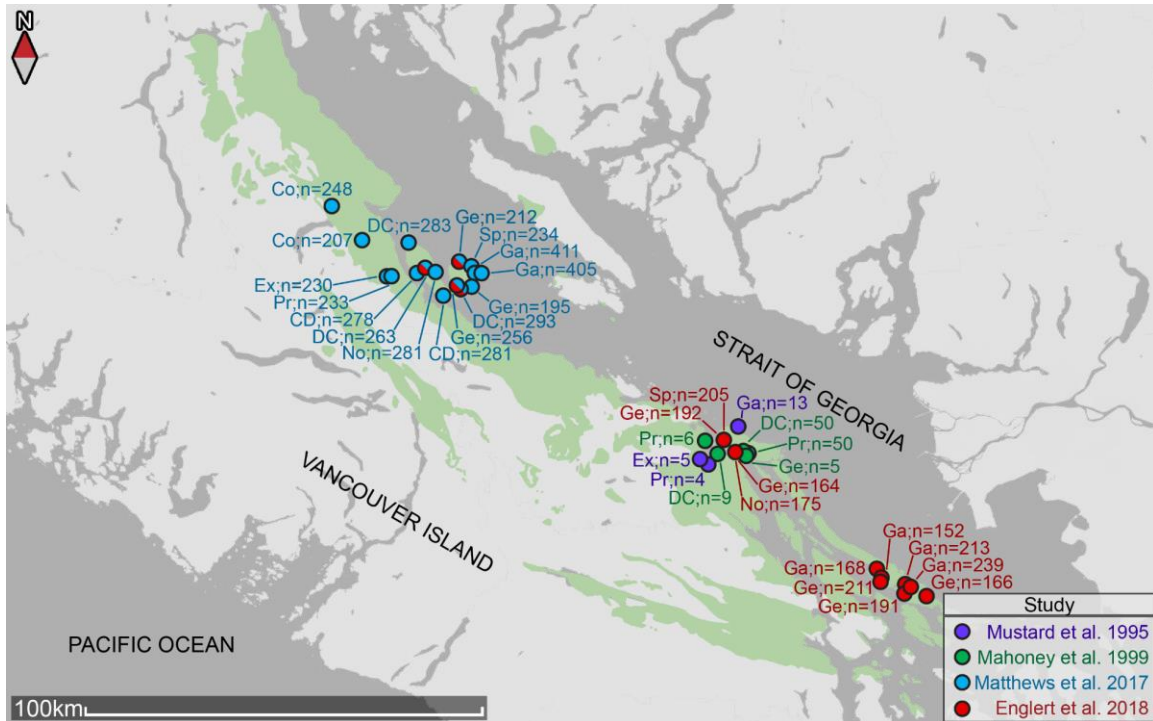


Figure 1.5 Previous published DZ data. For each sample, information is provided on lithostratigraphic formation of origin and grain count. For example, a DZ sample taken from the Comox Fm with 248 ages is recorded as (Co; n=248). Acronyms: Co = Comox Fm, Ex = Extension Fm, Pr = Protection Fm, CD = Cedar District Fm, DC = De Courcy, No = Northumberland Fm, Ge = Geoffrey, Sp = Spray, Ga = Gabriola. Samples are colour-coded by study.

1.6. Methodology

From 2015 to 2018, twenty-one high-n (n = 147 to 314) DZ samples were collected and analysed from lower Nanaimo Group strata in outcrops and core along a 200 km transect through the Nanaimo and Comox sub-basins (Fig. 1.6; Appendix C). Samples represent four of the five lower Nanaimo Group lithostratigraphic formations, and most samples were acquired from strata within 700 m of the basal unconformity. Each DZ sample was assigned a lithostratigraphic formation by comparison to published lithostratigraphic schemes and geological maps, and by comparing sedimentological and ichnological characteristics to formation descriptions of Mustard (1994).

Depositional environments were assigned to each DZ sample by facies analysis of the host strata (Appendix C; Jones 2016; Jones et al. 2018; Kent et al. in review). Strip logs displaying the location of DZ samples in core or outcrop are presented in Appendix D. Depositional environment interpretations are used to evaluate the effects of sediment-routing processes in each environment on the expression of source areas in DZ age distributions, and the potential for MDA to reflect true depositional age.

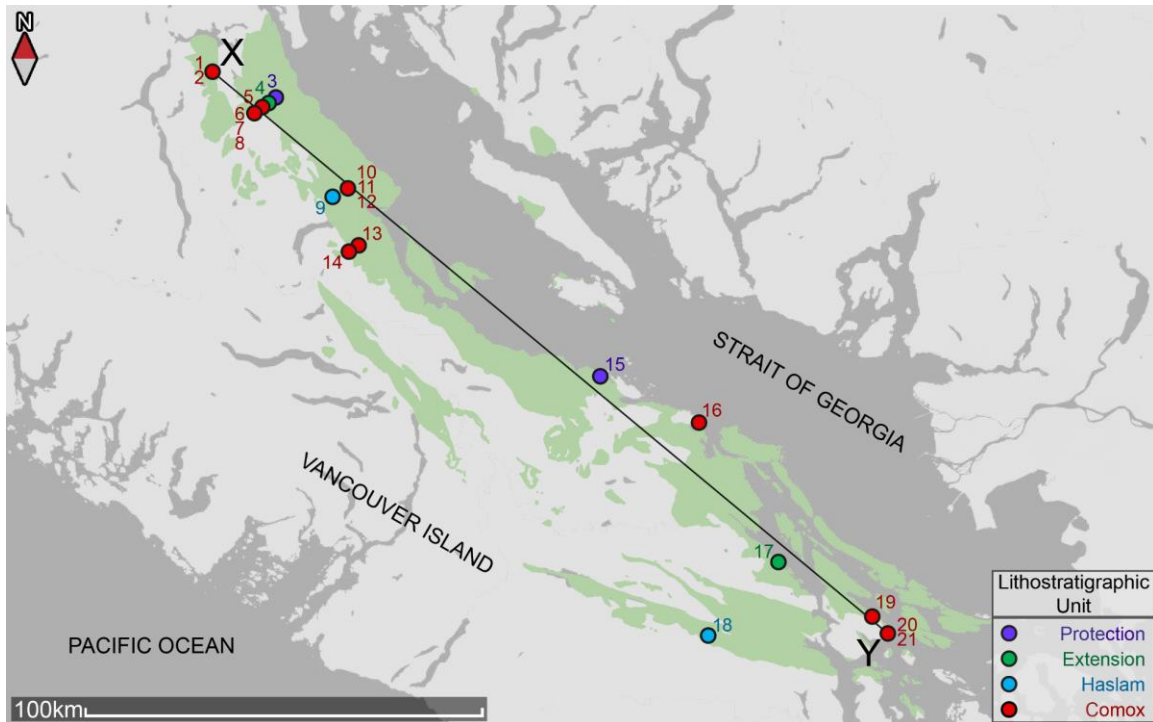


Figure 1.6 Sample sites for DZ samples published in this study. Colours indicate the lithostratigraphic unit from which a sample was taken. The line of section is depicted in Figure 3.2.

Three to five kg of sandstone were collected for each sample. Samples containing abundant living organic material such as algae and moss were subjected to nitric acid dissolution. Detrital zircons were isolated through a combination of mechanical crushing, Wilfley table separation, and methylene iodide heavy liquids separation at Simon Fraser University (SFU). Epoxy mounting and LA-ICP-MS U-Th-Pb dating was conducted at either the Center for Pure and Applied Tectonics and Thermochronology (CPATT), University of Calgary, Calgary, Alberta, Canada or Arizona LaserChron Center, University of Arizona, Tuscon, Arizona, USA.

Samples processed at CPATT were ablated using an ASI Resochron™ 193 nm excimer laser ablation system which incorporated a Laurin Technic M-50™ dual volume

cell. Isotopic signal intensities were measured using an Agilent 7700 quadrupole-ICP-MS. The ablation sequence employed a reference material-unknown bracketing procedure, with a measure of a FC1 zircon (Paces and Miller 1993) every 20 unknowns. Data reduction was accomplished in the Lolite™ (V2.5) software package (Patron et al. 2010) using the VizualAge data reduction scheme (Petrus and Kamber 2012). Finally, analyses with a probability of <1% concordance were eliminated from DZ datasets. Detailed analytical procedures for CPATT are available in Matthews and Guest (2017).

Ablation was conducted using a 193 nm New Wave Instruments™ and Lambda Physik™ Excimer laser ablation system. Isotopic signal intensities were measured using a GVI™ Isoprobe multicollector-ICP-MS. A Sri Lanka zircon was used to correct for elemental and isotopic fractionation (Gehrels 2000). Data reduction was conducted using an Excel spreadsheet (“agecalc”) equipped with VBA macros. No data filtering was applied. Detailed Arizona LaserChron Center procedures are available in Gehrels et al. (2008). Prior to their isotopic analysis, backscatter electron (BSE) and cathodoluminescence (CL) scanning electron microscope images were acquired on samples processed at Arizona LaserChron Center (Appendix A). Visible light images (Appendix B) are taken of the mounts prior to LA-ICP-MS. LA-ICP-MS datasets generated by each lab are available in Appendix C.

Data from LA-ICP-MS are imported into Density Plotter (Vermeesch 2012) and used to generate age distributions, which are presented as kernel-density estimations (KDEs), a statistical visualization technique that assumes a Gaussian distribution around each measured age but does not account for analytical uncertainties (Vermeesch 2012). Probability density plots (PDPs), which accounts for analytical uncertainties around each measured age (Vermeesch 2012), are also generated.

Age modes were selected using Age Pick 2010 (Gehrels 2010), and modes are displayed on the age distribution diagram if contributing grains represent more than 3% of the sample. Modes selected by Age Pick 2010 that were less than 5 Ma apart were merged, and a new mode was calculated by taking the weighted-average between the original modes.

Maximum depositional ages (MDAs) are calculated by taking the weighed-average of the three youngest grains overlapping at 2σ uncertainty (Y3G @ 2σ) using

the “Weighted Average” function of Isoplot 4.0 (Ludwig 2012) – all MDAs in this thesis use this technique unless otherwise mentioned. The use of Y3G @ 2σ is considered an acceptable compromise between using the youngest single grain (YSG), which yields a MDA closest to true depositional age but is irreproducible and subject to Pb-loss effects, and using the youngest three or more grain cluster overlapping at 2σ uncertainty (Y3G+ @ 2σ), which is statistically reliable but generates overly-conservative MDAs (Dickinson and Gehrels 2009). Additional MDA calculations using YSG and Y3G+ @ 2σ are presented in Appendix C. Facies-based correlations in the northern Comox Sub-Basin (Kent et al. in review) were favoured over DZ MDAs when determining the stratigraphic equivalency of local strata, as such correlations have been shown to reliably predict the distribution of coal seams in the area.

A multi-dimensional scaling plot (MDS) was generated using MuDiSc (Vermeesch 2013), a program which uses a table of pairwise “dissimilarities” between DZ samples to generate a plot in which samples with similar age modes are grouped together, and samples with dissimilar age modes are grouped apart. Detrital zircon samples clustering together on the MDS plot are interpreted to share similar source regions, whereas samples that were grouped apart were interpreted to have different provenances. The two-sample Kolmogorov-Smirnov statistic was used as a dissimilarity metric.

Chapter 2. Detrital zircon results and source areas

Detrital zircon from the lower Nanaimo Group (Comox, Haslam, Extension, Pender and Protection formations) yield 5,348 concordant dates from 21 samples. The majority of samples are dominated by Cretaceous grains, with modes around 150 and 90 Ma (Fig. 2.1; Appendix C). Excluding samples (S) 19–21, contribution of > 170 Ma grains is minor and averages 7.3% of the total. Maximum depositional ages for the 21 samples range from the Toarcian (Jurassic) to the Campanian (Fig. 2.2; Table 2; Appendix C), and MDS of the analyses yield four groups of similar DZ age distributions (Fig. 2.3).

Below, the DZ samples are described by MDA and MDS groupings. This is followed by a discussion of potential source areas. The chapter concludes with an evaluation of factors affecting the expression of MDAs and source areas in the DZ age spectra, and justifications for the disqualification of samples 16 and 19 from further analysis.

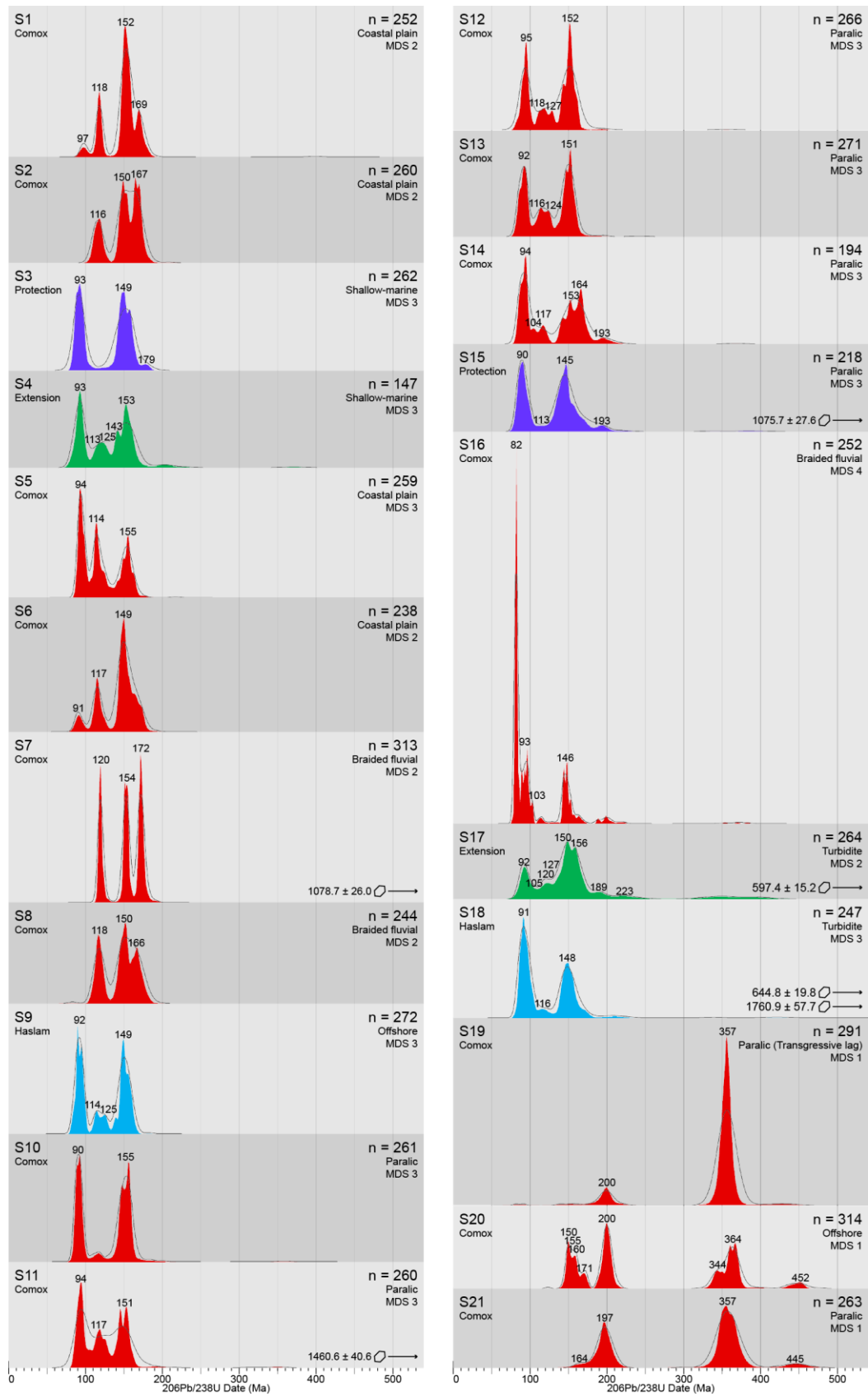


Figure 2.1 Normalized detrital zircon U-Pb spectra displayed as KDEs (filled) and PDPs (lines). Significant age modes (grains in that mode represent >3% of the sample) are labelled. Below the sample name are the lithostratigraphic formation. The “n” values at the far right are the number of concordant grains measured in each sample; below are interpreted depositional environment (Appendices C and D) and MDS group (Fig. 2.3). Y-axis is normalized probability. Kernel-density estimation plots are colour coded by formation using the same colour code as Figure 1.6. Red = Comox Fm, Blue = Haslam Fm, Green = Extension Fm, and Purple = Protection Fm.

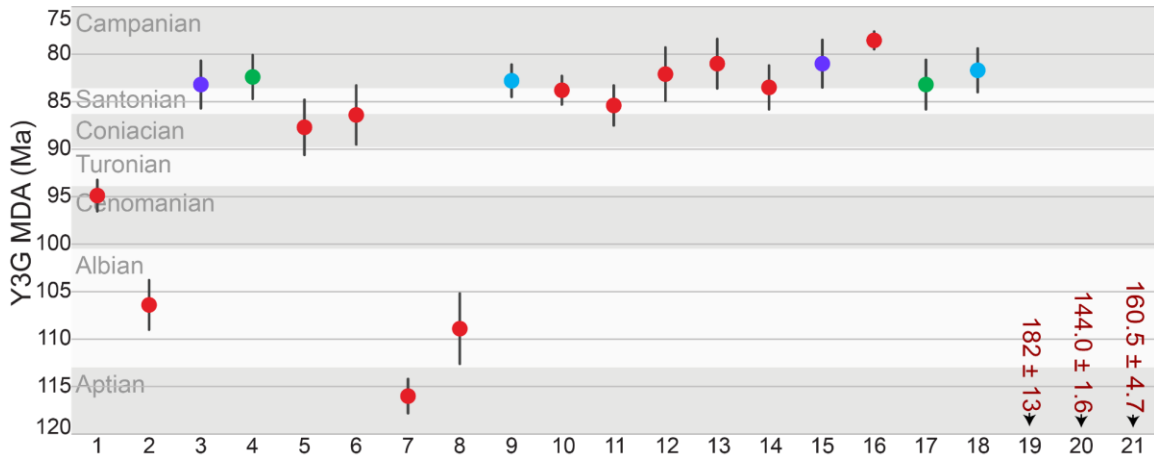


Figure 2.2 Plot of MDAs derived from samples. Sample number is shown on the x-axis and MDA on the y-axis. Coloured circles represent the MDA, and vertical lines show the uncertainty in ages. Maximum depositional ages are based on Y3G @ 2σ. The grey and white bands behind the samples shows the age range of the Geologic Age intervals (gray letters). Samples are colour coded by formation using the same colour code as Figure 1.6. Red = Comox Fm, Blue = Haslam Fm, Green = Extension Fm, and Purple = Protection Fm.

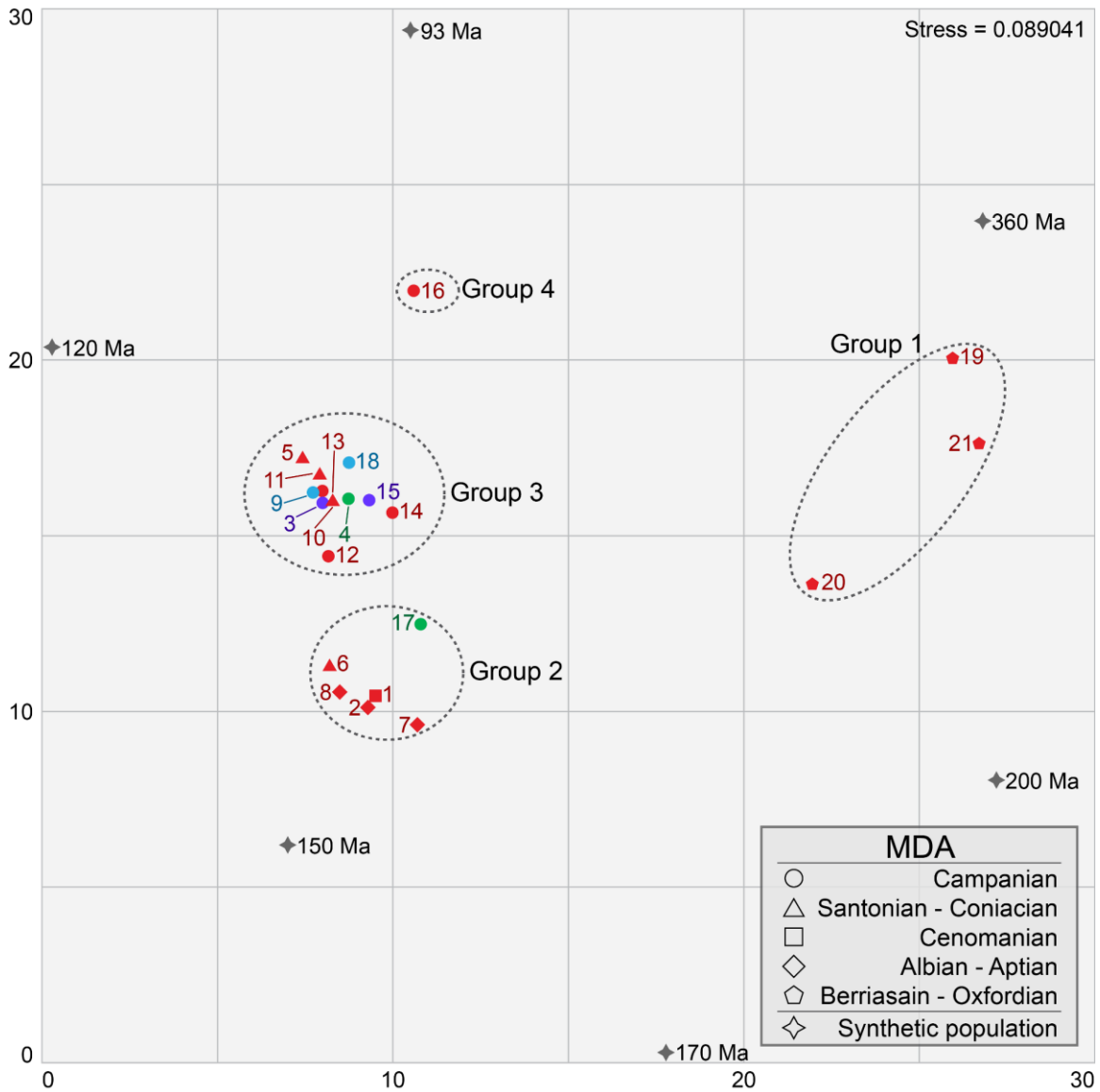


Figure 2.3 Two-sample non-metric Kolmogorov-Smirnov statistic MDS plot assessing similarities of DZ samples 1–21. Four MDS groups are defined based on nearest-neighbour analysis. Barring Group 4, DZ samples sharing a group have nearest neighbours which map to another member of the group. Artificial populations at 360, 200, 170, 150, 120 and 93 Ma are also provided; these ages represent the most prevalent modes in the DZ samples. A stress value of 0.089041 indicates that the 2-dimensional distances between samples displayed on the plot are a fair approximation of the multi-dimensional differences between samples (Kruskal 1964). Samples are colour coded by formation using the same colour code as Figure 1.6. Red = Comox Fm, Blue = Haslam Fm, Green = Extension Fm, and Purple = Protection Fm.

2.1. Maximum depositional ages

Maximum depositional ages show no correlation by lithoformation (Fig. 2.2). Comox Fm sample MDAs range over 100 Ma: from the Toarcian (S19; 182 ± 13 Ma) to the Campanian (S16; 78.55 ± 0.9 Ma). Stratigraphically higher samples from the Haslam, Extension, and Protection formations possess broadly coeval Campanian MDAs, and range from 83.2 ± 2.6 (S17) to 81.0 ± 2.5 Ma (S15).

2.2. Multi-dimensional scaling groups

Multi-dimensional scaling of DZ samples create 4 groups which vary as a function of MDA (Fig. 2.3), rather than lithoformation.

2.2.1. Group 1

Multi-dimensional scaling Group 1 (Fig. 2.3) includes three samples (S19–21), all of which are derived from strata assigned to the Comox Fm. Multi-dimensional scaling Group 1 samples are distinctive from all others derived from the lower Nanaimo Group, and include Jurassic (S19: 182 ± 13 ; S21: 160.5 ± 4.7 Ma) and earliest Cretaceous (S20: 144.0 ± 1.6 Ma; Fig. 2.2) MDAs. These samples are characterized by age modes at 200–197 Ma and 364–344 Ma (Fig. 2.1), both of which are rare in all other MDS groups. Samples 20 and 21 also contain a minor mode at 452–445 Ma.

2.2.2. Group 2

Multi-dimensional scaling Group 2 (Fig. 2.3) include six samples, five of which are derived from strata assigned to the Comox Fm (S1–2 and 6–8), and one from the Extension Fm (S17; Fig. 2.2). MDS Group 2 samples from the Comox Fm return MDAs from the Aptian (S7: 116.0 ± 1.8 Ma) through to the Coniacian (S6: 86.4 ± 3.1 Ma), and are characterized by a significant age mode at 154–150 Ma and variably sized modes at 120–116 Ma and 172–166 Ma (Fig. 2.1). Samples 1 and 6 also contain a minor 97–91 Ma age cluster. The MDS Group 2 sample from the Extension Fm (S17) returned an MDA from the Campanian (83.2 ± 2.6 Ma) and is characterized by major modes at 91 and 158–147 Ma. Sample 17 also contains a significant number of >180 Ma grains (16%).

2.2.3. Group 3

Multi-dimensional scaling Group 3 (Fig. 2.3) includes 11 samples, six of which are derived from the Comox Fm (S5 and 10–14), two from the Haslam Fm (S9 and 18), one from the Extension Fm (S4), and two from the Protection Fm (S3 and 15). Multi-dimensional scaling Group 3 samples from the Comox Fm return MDAs from the Coniacian (S5: 87.7 ± 2.9 Ma) to the Campanian (S13: 81.0 ± 2.6 Ma; Fig 4a), whereas samples from the Haslam, Extension, and Protection formations only have Campanian MDAs (S3: 83.2 ± 2.5 Ma to S15: 81.0 ± 2.5 Ma; Fig. 2.2). All MDS Group 3 samples are characterized by 94–91 Ma and 155–145 Ma age modes. MDS Group 3 samples also have variable contributions of 118–113 Ma grains with a notable decrease in the size of this contribution with younger MDA (Fig. 2.1). Samples 4, 11, 15, 16, and 18 have a relatively minor number of grains > 180 Ma (S4: 3% to S15: 6%).

2.2.4. Group 4

Multi-dimension scaling Group 4 (Fig. 2.3) comprises only Sample 16, derived from the Comox Fm. It yielded a Campanian MDA (78.6 ± 0.9 Ma; Fig. 2.2) and is characterized by a prominent 82 Ma age mode that is absent from all other DZ samples. Minor modes at 93, 103 and 146 Ma are also present, as well as a minor number of grains > 180 Ma (6%).

2.3. Source area interpretations

2.3.1. Coast plutonic complex

The nearby Coast Plutonic Complex (CPC) was a significant source of detritus for the Nanaimo Group, including broadly coeval DZ. This interpretation is supported by results from petrology, clast compositions, DZ geochronology, and paleocurrent analysis (Ward and Stanley 1982; Pacht 1984; Mustard 1994; Mustard et al. 1995; Mahoney et al. 1999; Matthews et al. 2017). Most DZ samples presented in this study possess modes that correspond to major periods of magmatic influx in the CPC.

The CPC was generated between 190 and 50 Ma as a result of continental arc magmatism; Mesozoic magmatism in the CPC is mostly related to Insular Belt accretion

along the former western margin of North America (Nelson 1979; Monger et al. 1982; Rusmore and Woodsworth 1991; Van der Heyden 1992; Gehrels et al. 2009; Mahoney et al. 2009). U-Pb ages of northern CPC plutons ($> 52^{\circ}$ N) reveal two mid-Mesozoic domains with unique magmatic histories (Fig. 2.4). These are separated by the Coast shear zone, a high angle lineament of Cretaceous to Eocene deformation. The western domain is characterized by two episodes of magmatism: one from 160–140 Ma period and another from 120–100 Ma. Magmatism progressed eastward through time, albeit with a major lull between 140–120 Ma. The eastern domain is instead characterized by continuous magmatism between 160–120 Ma, and a lull from 120–100 Ma (Gehrels et al. 2009; Mahoney et al. 2009). A third, 100–50 Ma domain overprints both older domains (Gehrels et al. 2009).

U-Pb, K-Ar, and Rb-Sr ages of southern CPC plutons (49 to 51° N) resemble that of the western domain of the northern CPC (Friedman and Armstrong 1995). Magmatism was pronounced in two periods: 170–145 Ma, and 125–65 Ma (Fig. 2.4). However, some characteristics of the western domain of the northern CPC are not as pronounced, such as a decrease in magmatism between 140–120 Ma and an eastward progression of magmatism from 120–100 Ma (Friedman and Armstrong 1995; Gehrels et al. 2009). There is also no Coast shear zone-equivalent structure in the southern CPC.

In this study, one Group 1 sample (S20) hosts multiple modes between 160–150 Ma. All Group 2 samples feature 156–149 and 116–120 Ma modes, two samples (S2 and 8) host a 167–166 Ma mode, and three (S1, 6 and 17) contain a 97–91 Ma mode. All Group 3 samples have prominent 155–145 Ma and 95–90 Ma modes, one (S14) hosts a 164 Ma mode, and most samples (S4, 5, 9, 11, 12, 13, 14, 15, 18) contain a 118–113 Ma mode. Detrital zircon ages within these modes are attributed to the CPC, as these time ranges correspond to periods of magmatism in arc. Additionally, these modes favour the southern CPC over the north, as 167–166 Ma precedes significant magmatism in the north but not the south (Friedman and Armstrong 1995; Gehrels et al. 2009).

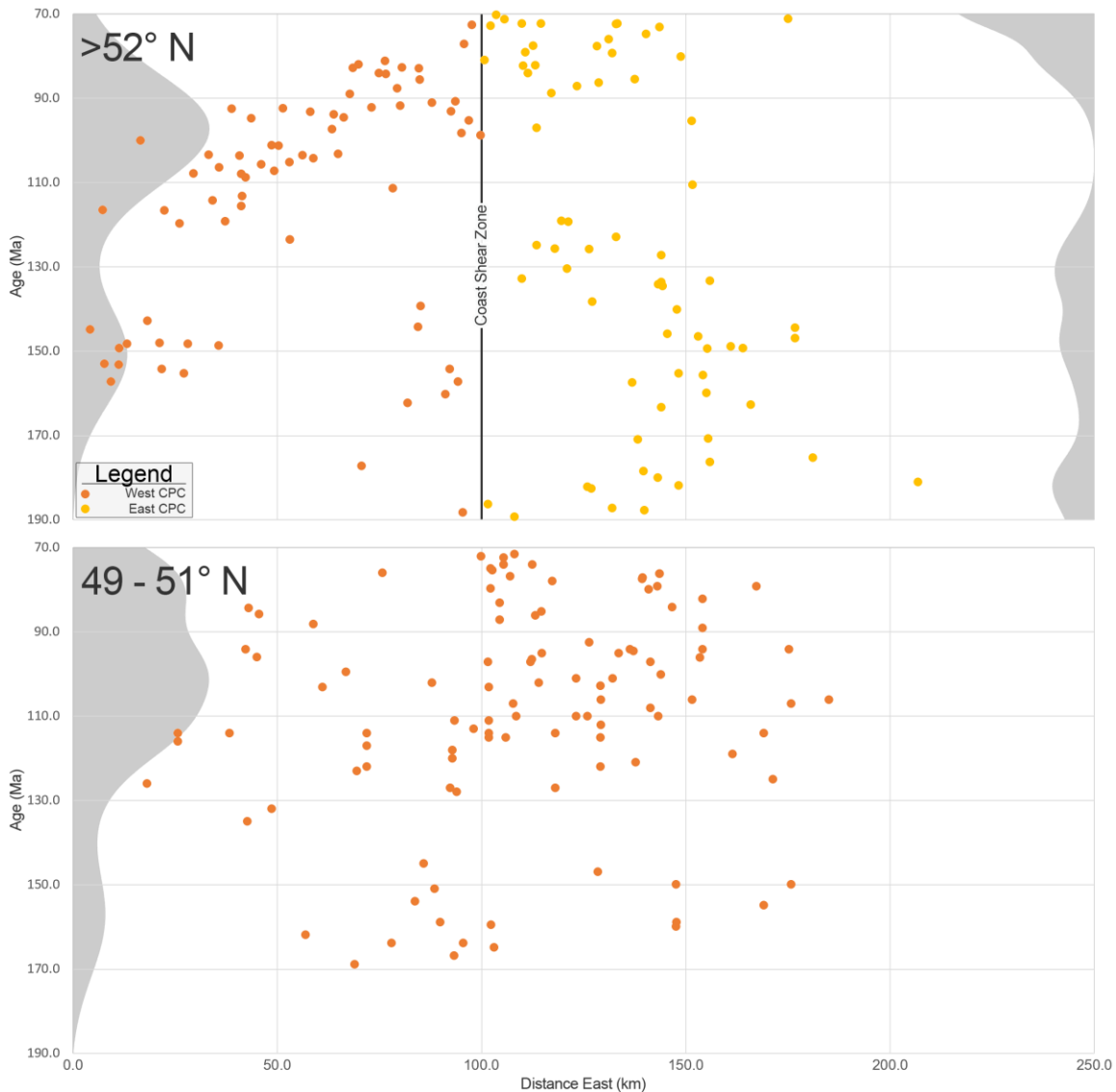


Figure 2.4 Dates of 190–70 Ma plutons from the northern (>52° N) and southern (49 to 51° N) CPC, and their magmatic fluxes over time. Distance in northern CPC is relative to the Coast shear zone, and distance in the southern CPC is relative to the Nanaimo Group. Each dot represents a single zircon or titanite age, and the filled grey curves are KDEs of plutons. Figure modified after Gehrels et al. (2009) and Matthews et al. (2017). Data for northern CPC is compiled from Gehrels et al. (2009) and data for the southern CPC is compiled from Friedman and Armstrong (1995).

Although volcanism occurred in the CPC during deposition of the Nanaimo Group, ash beds are unknown in all locales except for a tonstein in the northern Comox Sub-Basin along the Iron River (Kenyon et al. 1992). This is partially attributed to prevailing wind patterns along the western margin of North America ca. 100 Ma. Above 25° N, the predominantly east-trending westerlies (Stommel 1957; Lloyd 1982) would

have carried volcanic plumes from the CPC inland, and this is reflected in the distribution and thicknesses of ca. 90 Ma bentonite beds in the western interior of the United States, which suggest easterly and southeasterly transport from volcanic sources along the western paleo-North American margin (Elder 1988). While extensive ash deposits can be deposited upwind of eruptive events (Christiansen et al. 1994), accessible Nanaimo Group outcrops are located at least 30 km from the CPC – a long distance for volcanic plumes to travel against unbuffered winds from the paleo-Pacific ocean. It is possible that inaccessible lower Nanaimo strata underneath the Strait of Georgia contain abundant ash beds. Finally, ash layers will be rapidly reworked in depositional settings with high hydraulic energy, such as the paralic and braided fluvial environments common to much of the lower Nanaimo Group (Mustard 1994; Kent et al. in review).

2.3.2. Insular Belt sources

Detrital zircon modes older than 170 Ma are not attributed to the CPC, as these predate major magmatic episodes. These are instead attributed to various sources from the Insular Belt (Fig. 2.5).

Bonanza Arc

On Vancouver Island, the West Coast Crystalline Complex (WCC), Island Plutonic Complex (IPC), and Bonanza Group form three different crustal levels of the Jurassic Bonanza Arc (Isachsen 1987; DeBari et al. 1999; Canil et al. 2012), which is an island arc emplaced between 203–164 Ma (D'Souza et al. 2016). U-Pb analysis of the Bonanza Arc suggest pulses of magmatism at 198 and 171 Ma (D'Souza et al. 2016). In the modern, these rocks are exposed along the west coast and interior of Vancouver Island (Fig. 2.5), and underlie much of the Nanaimo Group (DeBari et al. 1999; Canil et al. 2012).

In this study, all Group 1 samples host a prominent 200–197 Ma mode, and one (S20) hosts a 171 Ma mode. A Group 2 sample (S17) hosts a 189 Ma mode and two (S1 and 7) host a 172–169 Ma mode. Two Group 3 samples (S14–15) host a 193 Ma mode, and one (S3) hosts a 179 Ma mode. Detrital zircon falling within these modes are attributed to the Bonanza Arc, as these time ranges correspond to periods of magmatism in arc.

Sicker Group

The Upper Devonian to Lower Permian Sicker Group comprises oceanic island arc volcanics and associated volcanoclastic assemblages, and represents the base of Wrangellia (Ruks 2015). U-Pb data suggest continuous volcanism from 365–335 Ma, and a pulse at 295 Ma (Ruks 2015). In the modern, the Sicker Group is exposed in four separated uplifts across Vancouver Island (Fig. 2.5). Uplift of the Sicker Group is attributed to Insular Belt accretion to North America during the Jurassic, and subsequent Eocene deformation related to the Cowichan fold and thrust belt (Muller 1980; England and Calon 1991; Ruks 2015).

In this study, all Group 1 samples host a 364–344 Ma mode. Detrital zircon falling within this mode are attributed to the Sicker Group, as this time range corresponds to a period of magmatism in the group.

Descon Arc

The Ordovician to Lower Silurian Descon arc comprises continental and oceanic arc volcanics and associated volcanoclastic assemblages, and belongs to the Alexander Terrane (Gehrels and Saleeby 1987; Nelson et al. 2010). U-Pb ages of cogenetic plutonic and hypabyssal rocks suggest periodic magmatism from 475–420 Ma (Gehrels and Saleeby 1987; Gehrels 1992). In the modern, these strata are exposed across the Alexander archipelago, in the Alaskan Panhandle (Fig. 2.5), 850 km northwest of the Georgia Basin.

In this study, all Group 1 samples host a 452–445 Ma mode. Detrital zircon falling within this mode are attributed to the Descon Arc, as this time range corresponds to a period of magmatism in the arc. While Ordovician DZ sources are present in Cascades terranes in close proximity to Nanaimo Group outcrops (Hoffnagle 2014; Schermer et al. 2018), the absence of Precambrian modes common to Cascades terranes in lower Nanaimo Group DZ age spectra precludes the Cascades terranes as a source region.

2.3.3. Other sources

Detrital zircon modes at 382, 245, 219, 209 Ma are present in samples collected from offshore and turbidite environments. A few Precambrian grains are also present. These are attributed to unknown sources and represent drainage from deep within the

North American continent, the nearby Cascade terranes, or long-distance transport along-shore.

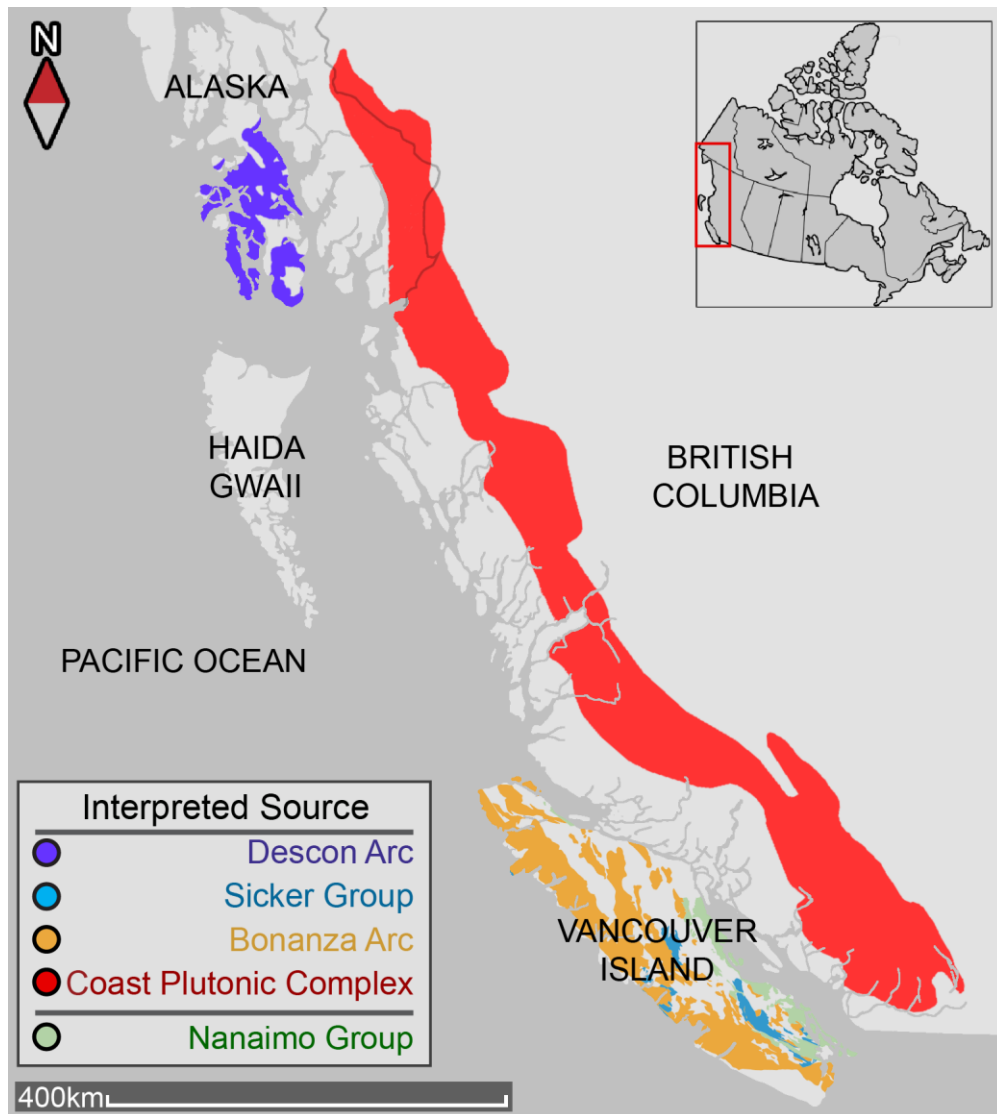


Figure 2.5 Modern outcrops of interpreted source areas. Modified from Wheeler and McFeely (1991).

2.4. Considerations for detrital zircon interpretations

Maximum depositional ages are used in this study to approximate true depositional age and infer temporal-equivalency of strata. Meanwhile, samples sharing an MDS group are interpreted to have common provenance. Because MDS groups vary by MDA, salient differences between groups are used to infer the evolution of source areas over time through processes such as uplift, erosion, and tectonic displacement.

DZ age spectra are affected by factors such as depositional environment (DeGraaf-Surpless et al. 2003; Sickmann et al. 2016), source area lithology (Spencer et al. 2018) and regional tectonics (Dickinson and Gehrels 2009). These physical aspects of the paleoenvironment must be taken into account prior to the usage of DZ to resolve stratigraphy and source area evolution.

2.4.1. Paleoenvironment

First, consideration should be given to the depositional environment of each sample (Appendices C and D), as each setting is subject to a set of hydraulic regimes which ultimately influence how DZ age spectra and their MDAs are expressed (DeGraaf-Surpless et al. 2003; Sickmann et al. 2016). Lower Nanaimo Group strata are deposited in 5 main depositional systems (Jones 2016; Jones et al. 2018; Kent et al. in review): braided fluvial (alluvial fans and braided rivers), coastal plain (meandering rivers and floodplains), paralic & shallow-marine (estuaries, tidal flats, deltas, beach-shorefaces and storm-dominated shelf), offshore and turbidite (turbidite channels and levees). With respect to the DZ samples, samples 7, 8 and 16 originate from braided fluvial deposits, samples 1, 2, 5 and 6 are from coastal plain deposits, samples 3, 4, 10–15, 19 and 21 are sourced from paralic and shallow-marine settings, samples 9 and 20 originate from offshore strata, and samples 17 and 18 were sampled from turbidite deposits (Appendices C and D).

The reliability of DZ datasets for generating both MDAs that reflect true depositional ages and age spectra that capture all source areas in a basin is lower for samples acquired from braided fluvial (S7, 8, 16) and coastal plain strata (S1, 2, 5, 6). Detrital zircon age spectra generated from braided fluvial and coastal plain settings will only reflect source areas in their associated catchments, leading to the possibility that a broadly coeval volcanic source supplying DZ close to true depositional age is unrepresented. This is best demonstrated by samples 7 and 8, which both originate from braided fluvial environments. Sample 8 yields an Albian MDA (108.9 ± 3.7 Ma; Fig. 2.2), despite being 50 m below S7 (Appendix D), which yields an Aptian MDA (116.0 ± 1.8 Ma; Fig. 2.2). This effect is more pronounced in braided fluvial environments than coastal plains, as coastal plains are distal to braided fluvial settings, and hence, tend to host sediment from a greater variety of source regions.

Detrital zircon MDAs taken from paralic, shallow-marine (S3, 4, 10–15, 19 and 21), offshore (S9 and 20) and turbiditic (S17 and 18) environments are more likely to approximate true depositional age, and age spectra are more likely represent all source areas feeding the basin. In shallow-marine environments, along-strike processes can contribute more than 35% of final depositional mass (Hampson et al. 2014), and hence, paralic samples should contain DZs from all catchments connected by littoral transport (Sickmann et al. 2016). Consequently, there is a higher likelihood of incorporating broadly coeval DZ from recent volcanic activity in the adjacent arc. Further, in many deep-marine environments, such as submarine canyons or shelves, sediments from multiple source areas are captured and mixed, further increasing the probability of incorporating the youngest zircon present in the depositional system. Additionally, DZ from sources with low rates of erosion are sequestered in such environments (Sickmann et al. 2016). For example, amongst samples possessing Santonian to Campanian MDAs (S3, 4, 9–18), there are increasing contributions of non-CPC DZ (age > 170 Ma) in increasingly seaward depositional environments. Paralic and shallow-marine samples possess just over half (4.1%) of such > 170 Ma DZ as offshore and turbidite samples (7.0%).

Finally, strata comprising transgressive lags (S19), are formed through the cannibalization of older strata. DZ samples taken from such environments do not accurately reflect the range of source areas available during active deposition. Although S19 possesses a Toarcian MDA (182 ± 13 Ma; Fig. 2.2), it also includes two grains of significantly younger age (79.3 ± 3.7 Ma and 95.6 ± 8.7 Ma; Appendix B). Consequently, S19 is interpreted to be at most Campanian in age. However, the 150 and 90 Ma modes which dominate other Campanian samples are absent, suggesting the transgressive cannibalization of a deposit with similar age modes to S21, rather than the deposition of detritus from actively shedding igneous or metamorphic source regions.

2.4.2. Magmatic quiescence

Strata deposited during magmatic lulls in the associated volcanic arc of a CMB are more likely to yield an MDA reflective of the last magmatic episode rather than true depositional age. This effect is likely more pronounced in depositional environments which do not mix sediment from multiple drainage basins, such as braided fluvial and coastal plains.

Barring MDS Group 1, the DZ in this study are interpreted to predominantly originate (average = 92.7%) from the southern CPC, which experienced magmatism from 170–145 Ma and 125–65 Ma, and a magmatic lull from 145–125 Ma (Friedman and Armstrong 1995). The majority of samples have Aptian or younger MDAs, meaning they were deposited during magmatic episodes. The only sample which was potentially deposited during a magmatic lull is S20, which has a Berriasian MDA (144.0 ± 1.6 Ma). However, magmatic quiescence does not mean a total absence of magmatism, as several plutons were emplaced in the southern CPC between 145–125 Ma (Fig. 2.3); as such, broadly coeval DZ from the CPC were likely in active circulation in the Georgia Basin from 145–125 Ma. Since S20 is derived from offshore strata (Appendices C and D), mixing processes such as storm waves (Sickmann et al. 2016) are likely to incorporate such broadly coeval DZ into the sample, albeit in limited amounts.

2.4.3. Paleogeography

Broadly coeval DZ can also be absent in a DZ sample due to changing paleogeography on an active margin. For example, S21 yields an Oxfordian MDA (160.5 ± 4.7 Ma; Fig. 2.2), and there is a paucity of grains with this age in the sample (Fig. 2.1; Appendix C). This does not indicate an absence of coeval volcanism during the Oxfordian, as this time was a period of active magmatism in the CPC (Friedman and Armstrong 1995; Gehrels et al. 2009). Further, a DZ sample (S20) collected 45 m up section contains a mode at 159 Ma, and this mode comprises 6.7% (Appendix C) of the sample. Rather, S21 likely did not incorporate zircons from coeval volcanic sources during deposition likely leading its MDA to be much older than the true depositional age.

In Jura-Cretaceous time, and prior to final accretion of the Insular Belt, extensive connected arc-basin systems lined the paleo-North American margin (Monger et al. 1994; Brown and Gehrels 2007; Sauer et al. 2016). The Georgia Basin is interpreted to be one such arc-basin system. Nanaimo Group strata comprising MDS Group 1 likely shared similar tectonic settings with other Jurassic strata along the North American margin, including the Kahiltna Assemblage of Alaska (Ridgway et al. 2002) and the Great Valley Forearc of California (Constenius et al. 2000). During the deposition of S21, sediment routing systems of the Georgia Basin were separate from that of North America, leading to an absence of broadly-coeval DZ from the CPC.

2.4.4. Sedimentation rate

Although using MDAs to determine the stratigraphic position of samples separated by 10s of Ma is justifiable, this technique is not recommended for distinguishing between samples with overlapping MDA uncertainties, especially in CMBs where sediment accumulation rates commonly exceed 1 km Ma^{-1} (Lin et al. 2003; Nagel et al. 2013; Ramirez et al. 2015). For example, the lower Nanaimo Group is estimated to be up to 1 200 m thick (Mustard 1994; Kent et al. in review), and hence, the entire succession could have accumulated in $< 1 \text{ Ma}$. In this study, samples from the Haslam, Extension and Protection formations possess MDAs with 2σ uncertainties that average 2.4 Ma, which is well below the resolution necessary to resolve the depositional architectures of the host strata (Fig. 2.2). As a result, DZ data must be groundtruthed through facies analysis and sequence-stratigraphic correlation (Kent et al. in review) to test their accuracy and reliability.

2.4.5. Sample reliability

Sample 16 is discounted from further provenance analysis, as it does not represent a reasonable proportion of source areas for the Georgia Basin at the time. Sample 19 is discounted from further MDA and provenance analysis, as its MDA does not represent true depositional age, and it does not accurately portray active igneous/metamorphic source areas for the Georgia Basin at the time.

Chapter 3. Revisions to the history of the Georgia Basin

3.1. A revised chronostratigraphy for the lower Nanaimo Group

The DZ data presented herein reveal a more complicated depositional history for the lower Nanaimo Group, Georgia Basin, than has been previously recognized. Specifically, lithostratigraphy can be erroneously taken to imply sequential deposition of formations, and vertical filling of the basin (e.g. Mustard 1994; McCarron 1997; Takashima et al. 2004; Aksoy et al. 2005). If such were the case, then DZ samples from the same formation should yield similar MDAs and be grouped together by MDS reflecting their similar age distributions. Further, stratigraphically higher formations should yield sequentially younger MDAs, and be grouped apart by MDS, reflecting their disparate age distributions.

Instead, MDAs reveal that the lithostratigraphic formations presently assigned to the lower Nanaimo Group are not time-correlative, and MDS of DZ samples reveal that strata assigned to the same formation are not always genetically related; rather, genetic affinity between strata is more related to geographic location, stratigraphic position, and MDA. As well, differences in age distributions between samples demonstrate that multiple sediment sources existed for the Georgia Basin, and that these changed over time (Table 3.1).

| Source area | DZ mode (Ma) | MDS Group 1 ~160 to 145 Ma | MDS Group 2 ~110 to 85 Ma | MDS Group 3 ~85 to 80 Ma |
|------------------------|--------------|-------------------------------|------------------------------|-----------------------------|
| Coast plutonic complex | 97–91 | | ○ | ● |
| | 120–113 | | ● | ○ |
| | 156–145 | ○ | ● | ● |
| | 167–160 | ○ | ○ | ○ |
| Bonanza Arc | 171–169 | ○ | ○ | ○ |
| | 200–189 | ● | ○ | ○ |
| Sicker Group | 364–344 | ● | | |
| Descon Arc | 452–445 | ● | | |

○ Some samples contain mode ● All samples contain mode

Table 3.1 Summary of source area changes between MDS Groups; samples 16 and 19 have been excluded as they do not reasonably portray the range of igneous/metamorphic source areas active during the deposition of their host strata.

The most problematic formation in terms of age and lithostratigraphic assignment is the Comox Fm. The Comox Fm is defined as the first coarse clastic unit directly overlying the basal nonconformity (Mustard 1994), and is assigned a Turonian to Santonian depositional age based on biostratigraphy (Haggart et al. 2005). Comox Fm MDAs instead extend from the Jurassic (Oxfordian (S21)) to the Upper Cretaceous (Campanian (S12, 13 and 16)), suggesting the existence of previously unknown disconformities, including a potential Turonian-Santonian hiatus in the Comox Sub-Basin (Figs. 3.1 and 3.2A) and a potential Jurassic-Turonian hiatus in the Nanaimo Sub-Basin (Fig. 3.2A). Comox Fm DZ samples also share affinities with all MDS groups rather than clustering by formation, reflecting differing point sources through both time and space (Table 3.1). Overlying the Comox Fm are the Haslam, Extension and Protection formations, all of which share similar MDAs and MDS affinities (Figs. 2.2 and 2.3). Some Comox Fm samples also show similar MDAs and age distributions (MDS Group 3) to the three overlying formations. The similar MDAs and age distributions of some Comox and all Haslam, Extension, and Protection formation samples suggest either very high sedimentation rates, and /or contemporaneous deposition of these lithostratigraphic units. Lower Nanaimo Group strata range up to 1,200 m thick (Mustard 1994; Kent et al. in review), and deposition is broadly accepted (based on biostratigraphy) to have extended from the start of the Turonian to the end of the lower Campanian. However, many lower Nanaimo Group outcrops are unfossiliferous, leading such locales to have uncertain stage assignments (Muller and Jeletzky 1970; Ward 1978). Convergent-margin basins commonly experience very rapid sediment accumulation rates (e.g., $> 2,200 \text{ m Ma}^{-1}$ in the Western Foreland Basin, Taiwan (Lin et al. 2003; Nagel et al. 2013); $> 1,650 \text{ m Ma}^{-1}$ in the Kumano Forearc Basin, Japan (Ramirez et al. 2015)), raising the possibility that lower Nanaimo Group strata have accumulated in a very short period of time ($< 1 \text{ Ma}$). This means DZ samples with similar MDAs could have wide stratigraphic separation. Alternatively, and perhaps in conjunction with high sedimentation rates, sequence stratigraphic reconstruction of the Comox Sub-Basin reveals that lithoformations that are interpreted as being deposited sequentially are, in fact, contemporaneous with each other; sequence stratigraphic correlations place samples 4 (Extension), 9 (Haslam), 10 and 13 (Comox) as being equivalent to each other (Fig. 3.1; Kent et al. in review).

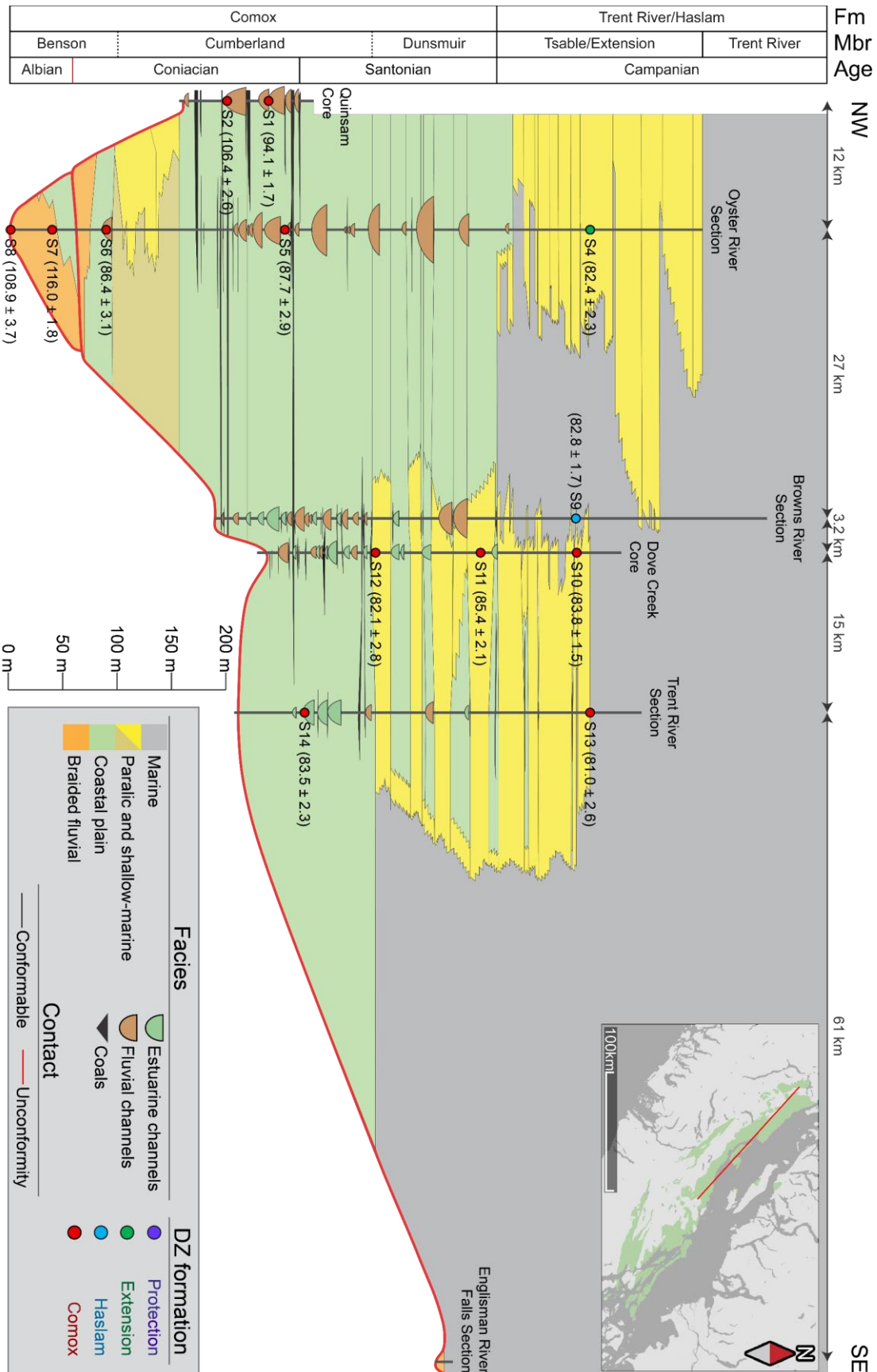
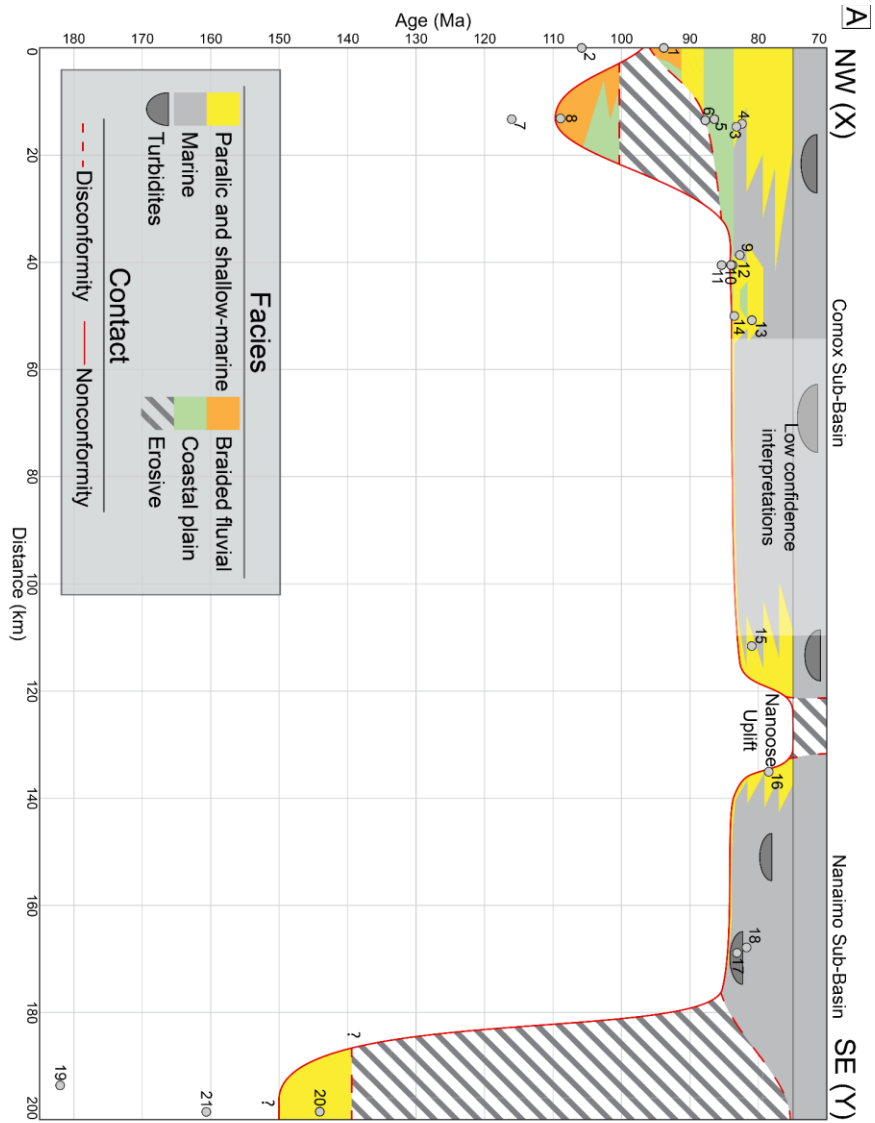


Figure 3.1 Interpreted sequence stratigraphy of the lower Nanaimo Group in the Comox Sub-Basin based on facies analysis, stratigraphic correlation and DZ MDAs (modified after Kent et al. (in review)). Strata are grouped into four depositional systems: braided-fluvial, coastal plain, paralic & shallow-marine, and marine. The position of DZ samples taken from the Comox Sub-Basin are shown on the vertical sections (vertical black lines). Acronyms: Formation = Fm; Member = Mbr.

An alternate view to the chronostratigraphy presently accepted in the Nanaimo Group (Mustard 1994), as well as to a single basin initiation event in the late Santonian/early Campanian (England and Bustin 1998), is that the Wrangellian basement underwent multiple phases of subsidence, deposition and uplift. This led to preservation of older strata in shallow sedimentary depressions, explaining the presence of Jura-Cretaceous strata in the Nanaimo Sub-Basin, and Albian strata in the Comox Sub-Basin (Fig. 3.2) and under the city of Vancouver (England and Bustin 1998).

A model based on variable subsidence and uplift explains the wide range of MDAs and age distributions present in the Comox Fm, as well as a potential Turonian-Coniacian hiatus in the Comox Sub-Basin (Fig. 3.1 and 3.2A) and a potential Berriasian-Turonian hiatus in the Nanaimo Sub-Basin (Fig. 3.2A). Three depositional episodes for the lower Nanaimo Group are interpreted on the basis of fieldwork, DZ MDAs, and MDS groupings: (1) Tithonian (Jurassic) to Berriasian; (2) Albian; and (3) Cenomanian to Campanian. Age spectra varying between DZ samples with different MDAs (Table 3.1) is attributed to tectonic events affecting source areas during hiatuses. Multiple episodes of subsidence in tectonically active regions are not uncommon, and have been documented previously in other CMBs such as Kahiltna backarc of Alaska (Ridgway et al. 2002) or the Great Valley forearc of California (Constenius et al. 2000). Together, the DZ results suggest a more complicated initiation to the Georgia Basin than has previously been described.



B Age Lithostratigraphic Formation

| | |
|---------------|---------------------|
| Maastrichtian | Upper Nanaimo Group |
| Campanian | Protection |
| Santonian | Pender |
| Coniacian | Extension |
| Turonian | Haslam |
| Cenomanian | Comox |
| Albanian | |
| Aptian | |
| Barremian | |
| Hauterivian | |
| Valanginian | |
| Berresian | |
| Tithonian | |
| Kimmeridgian | |
| Oxfordian | |
| Callovian | |
| Bathonian | |
| Bajocian | |
| Aalenian | |
| Toarcian | |
| Pliensbachian | |

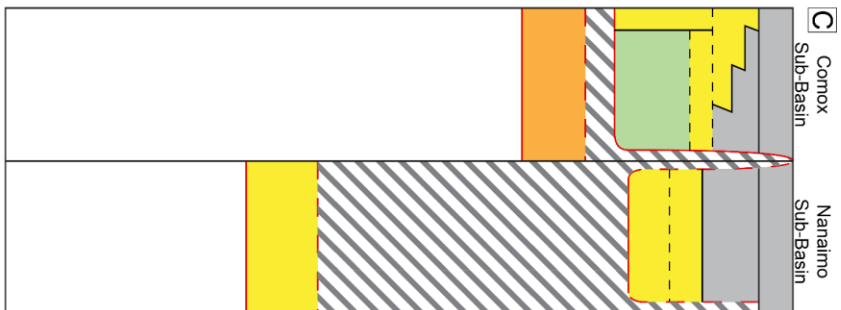


Figure 3.2 (A) Interpreted chronostratigraphy of the lower Nanaimo Group shown as a Wheeler Diagram for the Georgia Basin, based on DZ. Orange units are conglomerate dominated, green units are mudstone dominated, yellow units are sandstone dominated, and gray units are shale and mudstone dominated. The white area below the red line at the base of the Nanaimo Group represents both non-deposition and pre-Nanaimo Group strata (e.g., Jurassic volcanics) while the gray-hashed areas represent non-deposition / erosion within the Nanaimo Group. Circles and numbers indicate MDAs derived from DZ samples and sample numbers are given. The boundary between the lower and upper Nanaimo Groups is placed in the Campanian to reflect results from biostratigraphy (Ward 1978; Haggart et al. 2005). (B) Presently accepted chronostratigraphy of the Nanaimo Group (Ward 1978; Mustard 1994; Haggart et al. 2005). (C) Proposed chronostratigraphy for the lower Nanaimo Group in two sub-basins of the Georgia Basin, based on DZ geochronology. The colour of proposed stratigraphic units correlates to the dominant lithology. (A), (B) and (C) share the same time scale.

3.2. Implications for evolution of the Georgia Basin

In addition to implying a multi-phase subsidence and depositional history for the Georgia Basin, the DZ data suggest previously unknown tectonic translations and variable uplift of both the Wrangellian basement and CPC.

A small 452–445 Ma mode is present in MDS Group 1 samples, and the nearest probable source of these Ordovician grains is the Descon Arc (Gehrels and Saleeby 1987; Nelson et al. 2010), which is located on the Prince of Wales Island in the Alaskan Panhandle. This implies that the Georgia Basin was juxtaposed against the Descon Arc in Jura-Cretaceous time, and an 850 km sinistral displacement in the Lower Cretaceous is required to explain their modern arrangements. This is not unreasonable, as Lower Cretaceous sinistral displacements in the Coast and Insular Belts have been previously proposed by authors utilizing methods such as radioisotope dating of plutons, (Anderson and Silver 2005; Gehrels et al. 2009), and correlation of forearc, arc, and backarc assemblages (Monger et al. 1994).

The primary differences between MDS Groups 2 and 3 (Table 3.1) reflect variable exhaustion and uplift of source areas during the Upper Cretaceous. Specifically, in the CPC. The 156–145 Ma belt was topographic high from Albian to at least Campanian time, while the 120–113 and 167–160 Ma belts were uplifted in Albian time but became topographically insignificant by Campanian time. From 114–84 Ma, the

Coast Belt Thrust System emplaced a variety of westward propagating thrust stacks in the CPC (Brandon et al. 1988; Journeay and Friedman 1993; Umhoefer and Miller 1996; Brown and Gehrels 2007). Uplift of the 167–160, 156–145 and 120–113 Ma CPC magmatic belts in Albian time is attributed to this event. Meanwhile, continued contribution of 156–145 Ma CPC DZ in Campanian time reflects the location of continued thrust stack propagation coupled with burial/exhaustion of other magmatic belts.

Finally, MDS Groups 2 and 3 possess variable contributions from 364–344 and 200–197 Ma (Table 3.1) age modes, which correspond to periods of magmatism in the Sicker Group (Ruks 2015) and Bonanza Arc (DeBari et al. 1999; Canil et al. 2012; D'Souza et al. 2016), respectively. As both the Sicker Group and Bonanza Arc form part of the Wrangellian basement upon which the Nanaimo Group overlies (Mustard 1994; England and Bustin 1998), these results suggest limited exposure of the Wrangellian basement during deposition of the lower Nanaimo Group.

Chapter 4. Conclusions

A DZ geochronological study was conducted on the lower Nanaimo Group, in the Georgia Basin, Canada to assess the utility of its lithostratigraphic framework in a chronostratigraphic context. To achieve this the study aimed to determine if: (1) stratigraphically higher formations yield sequentially younger MDAs, and (2) if samples from the same formation yield similar provenance signatures.

From 2015 to 2018, twenty-one DZ samples were taken across the lower Nanaimo Group (Fig. 1.6). Most samples belong to the Comox Fm (Ward 1978; Mustard 1994) and are derived from strata in the Comox Sub-Basin (Fig. 1.6; England 1989). Samples were processed at Simon Fraser University, and dating was done by LA-ICP-MS either at CPATT, University of Calgary, Canada or Arizona LaserChron, University of Arizona, USA.

Maximum depositional ages show no correlation by formation, and MDS plots cluster samples by MDA rather than formation. This suggests that samples which share source areas have a common MDA, rather than a common lithostratigraphic origin. Furthermore, source areas for the Georgia Basin shifted with time.

Comox Fm samples are the most diverse in terms of MDA and provenance. Comox Fm samples possess MDAs that span over 80 Myr (S21: 160.5 ± 4.7 Ma to S16: 78.6 ± 0.9 Ma; Fig. 2.2) despite being correlated together lithostratigraphically. Multi-dimensional scaling (Fig. 2.3) assigns Comox Fm samples to four different groups, and samples from different MDS Groups yield distinctively different MDAs (Fig. 2.2), and are interpreted to have different source areas. The oldest samples (S7, 8 and 20 and 21) lie within 65 m of the basal unconformity, indicating the survival of older strata in probable paleo-topographic depressions. These results suggest that the Georgia Basin experienced multiple phases of subsidence and uplift, leading to the development of a basal unconformity with significant topography, and internal disconformities spanning millions of years. This is consistent with observations made in other forearc basins (Lin et al. 2003; Takano et al. 2013; Takano 2017) suggesting a common initiation mechanism for them. In addition, samples from stratigraphically higher units (Haslam, Extension and Protection formations) yield essentially contemporaneous MDAs (S15: 81.0 ± 2.5 Ma to S17: 83.2 ± 2.6 Ma; Fig. 2.2) and are grouped together by MDS (Fig.

2.3). The overlapping MDAs of Haslam, Extension and Protection formation MDAs and MDS is consistent with rapid sediment accumulation and coeval deposition of these strata, rather than sequential deposition. Indeed, sequence stratigraphic correlations in the Comox Sub-Basin assign stratigraphic equivalency to two Comox Fm (S10 and 13), one Haslam Fm (S9), and one Extension Fm (S4) samples.

This study highlights how DZ geochronology can be used to test and refine basin-scale stratigraphic frameworks, particularly in CMBs. In structurally complex CMBs and in unfossiliferous strata, DZ geochronology is an excellent method for resolving stratigraphic relations and depositional age when used in conjunction with sequence stratigraphy. However, several considerations must be taken into account when interpreting DZ data.

Detrital zircon MDAs from the lower Nanaimo Group are not universally reliable, especially when derived from braided fluvial and coastal plain samples. Source areas expressed in such environments are reflective only of the up-dip catchment (DeGraaf-Surpless et al. 2003; Sickmann et al. 2016), and hence, there is greater likelihood that a broadly coeval volcanic source is absent. Maximum depositional ages are more reliable when samples are derived from marine strata, as hydraulic processes such as long shore drift and storm wave reworking mix and transport sediment from all drainage catchments supplying a basin; this drastically increases the chance of a broadly coeval volcanic source being represented in the DZ population.

Although using MDAs to determine the stratigraphic position of samples separated by 10s of Ma is justifiable in some circumstances, this technique is not recommended for distinguishing between samples with overlapping MDA uncertainties, especially in CMBs where sediment accumulation rates commonly exceed 1 km Ma^{-1} (Lin et al. 2003; Nagel et al. 2013; Ramirez et al. 2015). This is exemplified in this study, in that the average 2σ uncertainty of MDAs is 2.4 Ma, which is well below the resolution necessary to resolve depositional architectures of Campanian-aged samples (Fig. 2.2). In such situations, a technique such as chemical abrasion-thermal ionization-mass spectrometry (CA-TIMS), which can achieve precisions better than 0.1% (Mattinson 2005), can be used on the youngest grains as determined by LA-ICP-MS to further resolve stratigraphic relationships.

4.1. Future work

The results presented suggest that initiation and subsidence of the Georgia Basin was much more complicated than previously thought. The data for this thesis will form the basis for (1) a revised architecture of the Georgia Basin's sedimentary fill and (2) a revised tectonic history for the Georgia Basin. Two steps would immediately make concrete progress towards these goals.

In this study, strata in Ruckle Park, Salt Spring Island, and along the Oyster River, Vancouver Island, yield Jura-Cretaceous and Albian MDAs, suggesting the potential preservation of older strata than previously described in the lower Nanaimo Group. However, DZ MDAs are not necessarily indicative of true depositional age, and are merely upper brackets (Dickinson and Gehrels 2009). Additional evidence from macro- and micro-fossil biostratigraphy will support or disprove the existence of much older strata within the Georgia Basin. The author of this thesis is unaware of index fossils that have been collected from either locality. Hence, additional fossils should be collected, utilizing precise taxonomy, and the accurate placement of first and last occurrences within the strata. The progressive development of more constrained assemblage zones is needed, utilizing all fossil groups and their ranges; however, precedence should be given to the presence of planktonic and nektonic organisms, which are independent of lithology. Further, verification of older strata through biostratigraphy would support the hypothesis that the Georgia Basin has undergone multiple phases of subsidence and sedimentation, and additional work could focus on resolving the tectonic environments within which older strata were emplaced. Evidence against the existence of older strata would also bracket tectonic evolution of the Georgia Basin, and suggest a single-episode of initiation and subsidence.

The existence of a 452–445 Ma mode in MDS Group 1 samples suggests that Wrangellia was juxtaposed against the Descon Arc during Jura-Cretaceous time, and a 850 km sinistral displacement of Wrangellia relative to the Insular Belt occurred during Lower Cretaceous time. Additional work to confirm such a displacement could involve using a technique such as Hafnium–Oxygen isotopes and trace element petrochronology to fingerprint zircon derived from the Descon Arc, and comparing them to Ordovician DZ found in MDS Group 1 samples. This would provide paleogeographic

constraints on the location of the Georgia Basin relative to North America and the Insular Belt during Lower Cretaceous time.

Ultimately, developing a revised architecture of the sedimentary fill, and a revised tectonic model for the Georgia Basin would yield insights into Mesozoic evolution of the western North American margin, and create a potentially useful analog for the evolution of CMBs worldwide.

References

- AGUE, J.J., AND BRANDON, M.T., 1996, Regional tilt of the Mount Stuart batholith, Washington, determined using aluminum-in-hornblende barometry: Implications for northward translation of Baja British Columbia: Geological Society of America Bulletin, v. 108, p. 471 - 488.
- AKSOY, E., TÜRKMEN, İ., AND TURAN, M., 2005, Tectonics and sedimentation in convergent margin basins: an example from the Tertiary Elazığ basin, Eastern Turkey: Journal of Asian Earth Sciences, v. 25, p. 459 - 472.
- ANDERSON, T.H., AND SILVER, L.T., 2005, The Mojave-Sonora megashear - Field and analytical studies leading to the conception and evolution of the hypothesis, *in* Anderson, T.H., Nourse, J.A., McKee, J.W., and Steiner, M.B., eds., The Mojave-Sonora megashear hypothesis: Development, assessment, and alternatives: Geological Society of America Special Paper, p. 1 - 50.
- BAIN, H.A., AND HUBBARD, S.M., 2016, Stratigraphic evolution of a long-lived submarine channel system in the Late Cretaceous Nanaimo Group, British Columbia, Canada: Sedimentary Geology, v. 337, p. 113 - 132.
- BECK JR., M.E., AND HOUSEN, B.A., 2003, Absolute velocity of North America during the Mesozoic from paleomagnetic data: Tectonophysics, v. 377, p. 33 - 54.
- BECK, M.E., AND NOSON, L., 1972, Anomalous Palaeolatitudes in Cretaceous Granitic Rocks: Nature Physical Science, v. 235, p. 11 - 13.
- BICKFORD, C.G.C., AND KENYON, C., 1988, Coalfield geology of eastern Vancouver Island: British Columbia Ministry of Energy, Mines and Petroleum Resources, Geological Fieldwork, v. 1988-1, p. 441 - 450.
- BRANDON, M.T., COWAN, D.S., AND VANCE, J.A., 1988, San Juan Thrust System, San Juan Islands, Washington: Geological Society of America Special Paper, v. 221, p. 81.
- BROWN, E., H., AND GEHRELS, G.E., 2007, Detrital zircon constraints on terrane ages and affinities and timing of orogenic events in the San Juan Islands and North Cascades, Washington: Canadian Journal of Earth Sciences, v. 44, p. 1375 - 1396.
- BUCKHAM, A.F., 1947, The Nanaimo Coal Field: Transactions of the Canadian Institute of Mining and Metallurgy, v. 50, p. 460 - 472.
- CANIL, D., JOHNSTON, S.T., LAROCQUE, J., FRIEDMAN, R.M., AND HEAMAN, L.M., 2012, Age, construction, and exhumation of the midcrust of the Jurassic Bonanza arc, Vancouver Island, Canada: Lithosphere, v. 5, p. 82 - 91.

- CAWOOD, P.A., HAWKESWORTH, C.J., AND DHUIME, B., 2012, Detrital zircon record and tectonic setting: *Geology*, v. 40, p. 875 - 878.
- CHRISTIANSEN, E.H., KOWALLIS, B.J., AND BARTON, M.D., 1994, Temporal and spatial distribution of volcanic ash in Mesozoic sedimentary rocks of the western interior: an alternative record of Mesozoic magmatism, *in* Caputo, M.V., Peterson, J.A., and Francyk, K.J., eds., *Mesozoic Systems of the Rocky Mountain Region, USA, The Rocky Mountain Section SEPM*.
- CLAPP, C.H., 1911, *Geology of the Victoria and Saanich Quadrangles, Vancouver Island, B.C.: Geological Survey of Canada, Summary Report*, v. 1910, p. 102 - 109.
- CLAPP, C.H., 1912, *Southern Vancouver Island: Geological Survey of Canada Memoir*.
- CLAPP, C.H., 1914, *Geology of the Nanaimo Map-Area: Geological Survey, Department of Mines Memoir*, v. 51, p. 135.
- CLOWES, R.M., BRANDON, M.T., GREEN, A.G., YORATH, C.J., BROWN, A.S., KANASEWICH, E.R., AND SPENCER, C., 1987, LITHOPROBE - souther Vancouver Island: Cenozoic subduction complex imaged by deep seismic reflections: *Canadian Journal of Earth Sciences*, v. 24, p. 31 - 51.
- CONEY, P.J., 1978, Mesozoic-Cenozoic Cordilleran plate tectonics: *Geological Society of America Memoir*, v. 152, p. 33 - 50.
- CONSTENIUS, K.N., JOHNSON, R.A., DICKINSON, W.R., AND WILLIAMS, T.A., 2000, Tectonic evolution of the Jurassic–Cretaceous Great Valley forearc, California: Implications for the Franciscan thrust-wedge hypothesis: *GSA Bulletin*, v. 112, p. 1703 - 1723.
- D'SOUZA, R.J., CANIL, D., AND CREASER, R.A., 2016, Assimilation, differentiation, and thickening during formation of arc crust in space and time: The Jurassic Bonanza arc, Vancouver Island, Canada: *GSA Bulletin*, v. 128, p. 543 - 557.
- DEBARI, S.M., ANDERSON, R.G., AND MORTENSEN, J.K., 1999, Correlation among lower to upper crustal components in an island arc: the Jurassic Bonanza arc, Vancouver Island, Canada: *Canadian Journal of Earth Sciences*, v. 36, p. 1371 - 1413.
- DEGRAAF-SURPLESS, K., MAHONEY, J.B., WOODEN, J.L., AND MCWILLIAMS, M.O., 2003, Lithofacies control in detrital zircon provenance studies: Insights from the Cretaceous Methow basin, southern Canadian Cordillera: *GSA Bulletin*, v. 115, p. 889 - 915.
- DICKINSON, W.R., AND GEHRELS, G.E., 2009, Use of U-Pb ages of detrital zircons to infer maximum depositional ages of strata: A test against a Colorado Plateau Mesozoic database: *Earth and Planetary Science Letters*, v. 288, p. 115 - 125.

- ELDER, W.P., 1988, Geometry of Upper Cretaceous bentonite beds: Implications about volcanic source areas and paleowind patterns, western interior, United States: *Geology*, v. 16, p. 835 - 838.
- ENGLAND, T.D.J., 1989, Late Cretaceous to Paleogene evolution of the Georgia Basin, Southwestern British Columbia: Memorial University, St. John's, 560 p.
- ENGLAND, T.D.J., AND BUSTIN, R.M., 1998, Architecture of the Georgia Basin southwestern British Columbia: *Bulletin of Canadian Petroleum Geology*, v. 46, p. 288 - 320.
- ENGLAND, T.D.J., AND CALON, T.J., 1991, The Cowichan fold and thrust system, Vancouver Island, southwestern British Columbia: *Geological Society of America Bulletin*, v. 103, p. 336 - 362.
- ENGLERT, R.G., HUBBARD, S.M., COUTTS, D.S., AND MATTHEWS, W.A., 2018, Tectonically controlled initiation of contemporaneous deep-water channel systems along a Late Cretaceous continental margin, western British Columbia, Canada: *Sedimentology*, p. 35.
- ENKIN, R.J., BAKER, J., AND MUSTARD, P.S., 2001, Paleomagnetism of the Upper Cretaceous Nanaimo Group, southwestern Canadian Cordillera: *Canadian Journal of Earth Sciences*, v. 38, p. 1403 - 1422.
- FRIEDMAN, R.M., AND ARMSTRONG, R.L., 1995, Jurassic and Cretaceous geochronology of the southern Coast Belt, British Columbia, 49° to 51°N, *in* Miller, D.M., and Busby, C., eds., *Jurassic Magmatism and Tectonics of the North American Cordillera*, Geological Society of America Special Paper, p. 95 - 139.
- GEHRELS, G.E., 1992, Geologic map of southern Prince of Wales Island, Southeastern Alaska, *in* Survey, U.S.G., ed., *IMAP*.
- GEHRELS, G.E., 2000, Introduction to detrital zircon studies of Paleozoic and Triassic strata in western Nevada and northern California, *in* Soreghan, M., and Gehrels, G.E., eds., *Paleozoic and Triassic Paleogeography and Tectonics of Western Nevada and Northern California*, Special Paper - Geological Society of America, p. 18.
- GEHRELS, G.E., 2010, Analysis tools.
- GEHRELS, G.E., RUSMORE, M., WOODSWORTH, G., CRAWFORD, M., ANDRONICOS, C., HOLLISTER, L., PATCHETT, J., DUCEA, M., BUTLER, R., KLEPEIS, K., DAVIDSON, C., FRIEDMAN, R.M., HAGGART, J.W., MAHONEY, J.B., CRAWFORD, W., PEARSON, D., AND GIRARDI, J., 2009, U-Th-Pb geochronology of the Coast Mountains batholith in north-coastal British Columbia: Constraints on age and tectonic evolution: *GSA Bulletin*, v. 121, p. 1341 - 1361.
- GEHRELS, G.E., AND SALEEBY, J.B., 1987, Geologic framework, tectonic evolution, and displacement history of the Alexander Terrane: *Tectonics*, v. 6, p. 151 - 173.

- GEHRELS, G.E., VALENCIA, V.A., AND RUIZ, J., 2008, Enhanced precision, accuracy, efficiency, and spatial resolution of U-Pb ages by laser ablation-multicollector-inductively coupled plasma-mass spectrometry: *Geochemistry Geophysics Geosystems*, v. 9, p. 13.
- HAGGART, J.W., WARD, P.D., AND ORR, W., 2005, Turonian (Upper Cretaceous) lithostratigraphy and biochronology, southern Gulf Islands, British Columbia, and northern San Juan Islands, Washington State: *Canadian Journal of Earth Sciences*, v. 42, p. 2001-2020.
- HAMBLIN, A.P., 2012, Upper Cretaceous Nanaimo Group of Vancouver Island as a potential bedrock aquifer zone: summary of previous literature and concepts: *Geol. Surv. Can*, v. Open File 7265, p. 20.
- HAMPSON, G.J., DULLER, R.A., PETTER, A.L., ROBINSON, R.A.J., AND ALLEN, P.A., 2014, Mass-balance constraints on stratigraphic interpretation of linked alluvial-coastal-shelfal deposits from source to sink: example from Cretaceous Western Interior Basin, Utah and Colorado, U.S.A: *Journal of Sedimentary Research*, v. 84, p. 935 - 960.
- HOFFNAGLE, E.A., 2014, Age, origin, and tectonic evolution of the Yellow Aster Complex: northwest Washington state: *Western Washington University*, 154 p.
- ISACHSEN, C.E., 1987, Geology, geochemistry, and cooling history of the Westcoast Crystalline Complex and related rocks, Meares Island and vicinity, Vancouver Island, British Columbia: *Canadian Journal of Earth Sciences*, v. 24, p. 2047 - 2064.
- JONES, M.T., 2016, Stratigraphy and architecture of shallow-marine strata on an active margin, lower Nanaimo Group, Vancouver Island, BC: *Simon Fraser University*.
- JONES, M.T., DASHTGARD, S.E., AND MACEACHERN, J.A., 2018, A model for the preservation of thick, transgressive shoreline successions: examples from the forearc Nanaimo Basin, British Columbia, Canada: *Journal of Sedimentary Research*, v. 88, p. 811 - 826.
- JOURNEY, J.M., AND FRIEDMAN, R.M., 1993, The Coast Belt Thrust system: Evidence of shortening in the Coast Belt of southwestern British Columbia: *Tectonics*, v. 12, p. 756 - 775.
- JOURNEY, J.M., AND MORRISON, J., 1999, Field investigation of Cenozoic structures in the northern Cascadia forearc, southwestern British Columbia: *Geological Survey of Canada, Current Research*, v. A, p. 239 - 250.
- KENT, B.A.P., HUANG, C., DASHTGARD, S.E., AND CATHYL-HUHN, G., in review, Initiation and Early Evolution of a Forearc Basin: *Georgia Basin, Canada*.

- KENYON, C., BICKFORD, C.G.C., AND HOFFMAN, G., 1992, Quinsam and Chute Creek Coal Deposits (NTS 92F/13, 14): British Columbia Ministry of Mines and Petroleum Resources, v. Paper 1991-3, p. 90.
- KIM, B., AND KODAMA, K.P., 2004, A compaction correction for the paleomagnetism of the Nanaimo Group sedimentary rocks: Implications for the Baja British Columbia hypothesis: *Journal of Geophysical Research*, v. 109, p. 1 - 17.
- KRIJGSMAN, W., AND TAUXE, L., 2006, E/I corrected paleolatitudes for the sedimentary rocks of the Baja British Columbia hypothesis: *Earth and Planetary Science Letters*, v. 242, p. 205 - 216.
- KRUSKAL, J., 1964, Multidimensional scaling by optimizing goodness of fit to a nonmetric hypothesis: *Psychometrika*, v. 29, p. 1 - 27.
- LIN, A.T., WATTS, A.B., AND HESSELBO, S.P., 2003, Cenozoic stratigraphy and subsidence history of the South China Sea margin in the Taiwan region: *Basin Research*, v. 15, p. 453 - 478.
- LLOYD, C.R., 1982, The Mid-Cretaceous Earth: Paleogeography; Ocean Circulation and Temperature; Atmospheric Circulation: *The Journal of Geology*, v. 90, p. 393 - 413.
- LUDWIG, K.R., 2012, A Geochronological Toolkit for Microsoft Excel, Isoplot/Ex, Rev. 3.75, Berkeley Geochronology Center.
- MAHONEY, J.B., GORDEE, S.M., HAGGART, J.W., FRIEDMAN, R.M., DIAKOW, L.J., AND WOODSWORTH, G.J., 2009, Magmatic evolution of the eastern Coast Plutonic Complex, Bella Coola region, west-central British Columbia: *GSA Bulletin*, v. 121, p. 1362 - 1380.
- MAHONEY, J.B., MUSTARD, P.S., HAGGART, J.W., FRIEDMAN, R.M., FANNING, C.M., AND MCNICOLL, V.J., 1999, Archean zircons in Cretaceous strata of the western Canadian Cordillera: The "Baja BC" hypothesis fails a "crucial test": *Geology*, v. 27, p. 195-198.
- MATTHEWS, W.A., AND GUEST, B., 2017, A practical approach for collecting large-n detrital zircon U-Pb data sets by quadrupole LA-ICP-MS: *Geostandards and Geoanalytical Research*, v. 41, p. 161 - 180.
- MATTHEWS, W.A., GUEST, B., COUTTS, D., BAIN, H.A., AND HUBBARD, S.M., 2017, Detrital zircons from the Nanaimo basin, Vancouver Island, British Columbia: An independent test of Late Cretaceous to Cenozoic northward translation: *Tectonics*, v. 36, p. 854 - 876.
- MATTINSON, J.M., 2005, Zircon U-Pb chemical abrasion ("CA-TIMS") method: Combined annealing and multi-step partial dissolution analysis for improved precision and accuracy of zircon ages: *Chemical Geology*, v. 220, p. 47 - 66.

- MCCARRON, J.J., 1997, A unifying lithostratigraphy of late Cretaceous-early Tertiary fore-arc volcanic sequences on Alexander Island, Antarctica: *Antarctic Science*, v. 9, p. 209 - 220.
- MCGUGAN, A., 1962, Upper Cretaceous foraminiferal zones, Vancouver Island, British Columbia, Canada: *Journal of the Alberta society of petroleum geologists*, v. 10, p. 585 - 592.
- MCGUGAN, A., 1979, Biostratigraphy and paleoecology of Upper Cretaceous (Campanian and Maestrichtian) foraminifera from the Upper Lambert, Northumberland, and Spray Formations, Gulf Islands, British Columbia, Canada: *Canadian Journal of Earth Sciences*, v. 16, p. 2263 - 2274.
- MCGUGAN, A., 1982, Upper Cretaceous (Campanian and Maestrichtian) Foraminifera from the Upper Lambert and Northumberland Formations, Gulf Islands, British Columbia, Canada: *Micropaleontology*, v. 28, p. 399 - 430.
- MCGUGAN, A., 1990, Upper Cretaceous (Santonian-lower Campanian) foraminiferal biostratigraphy of the Nanaimo Group, subsurface of the Parksville area, eastern Vancouver Island: *Bulletin of Canadian Petroleum Geology*, v. 38, p. 28 - 38.
- MONGER, J.W.H., 1997, Plate Tectonics and Northern Cordilleran Geology: An Unfinished Revolution: *Geoscience Canada*, v. 24, p. 189 - 198.
- MONGER, J.W.H., PRICE, R.A., AND TEMPELMAN-KLUIT, D.J., 1982, Tectonic accretion and the origin of the two major metamorphic and plutonic welts in the Canadian Cordillera: *Geology*, v. 10, p. 70 - 75.
- MONGER, J.W.H., VAN DER HEYDEN, P., JOURNEYAY, J.M., EVENCHICK, C.A., AND MAHONEY, J.B., 1994, Jurassic-Cretaceous basins along the Canadian Coast Belt: Their bearing on pre-mid-Cretaceous sinistral displacements: *Geology*, v. 22, p. 175 - 178.
- MULLER, J.E., 1980, The Paleozoic Sicker Group of Vancouver Island, British Columbia: *Geological Survey of Canada: Paper*, v. 79-30, p. 23.
- MULLER, J.E., AND JELETZKY, J.A., 1970, Geology of the Upper Cretaceous Nanaimo Group, Vancouver Island and Gulf Islands, British Columbia, Geological Survey of Canada; Department of Energy, Mines and Resources.
- MUSTARD, P.S., 1994, The Upper Cretaceous Nanaimo Group, Georgia Basin: Geology and geological hazards of the Vancouver region, southwestern British Columbia. Edited by JWH Monger. Geological Survey of Canada, Bulletin, v. 481, p. 27-95.
- MUSTARD, P.S., PARRISH, R.R., AND MCNICOLL, V., 1995, Provenance of the Upper Cretaceous Nanaimo Group, British Columbia: evidence from U-Pb analyses of detrital zircons: *Stratigraphic Evolution of Foreland Basins, SEPM Special Publication*, v. 52, p. 65 - 76.

- NAGEL, S., CASTELLORT, S., WETZEL, A., WILLETT, S.D., MOUTHEREAU, F., AND LIN, A.T., 2013, Sedimentology and foreland basin paleogeography during Taiwan arc continent collision: *Journal of Asian Earth Sciences*, v. 62, p. 180 - 204.
- NELSON, J.A., 1979, The western margin of the Coast Plutonic Complex on Hardwicke and West Thurlow Islands, British Columbia: *Canadian Journal of Earth Sciences*, v. 16, p. 116 - 1175.
- NELSON, J.L., DIAKOW, L.J., MAHONEY, J.B., GEHRELS, G.E., PECHA, M., AND VAN STAAL, C., 2010, Geology and Mineral Potential of the Southern Alexander Terrane and western Coast Plutonic Complex near Klemtu, Northwestern British Columbia: *Geological Fieldwork 2010*, v. Paper 2011-1, p. 73 - 98.
- PACES, J.B., AND MILLER, J.D., 1993, Precise U-Pb ages of Duluth Complex and related mafic intrusion, northeastern Minnesota: Geochronological insights to physical, petrogenetic, paleomagnetic, and tectonomagmatic processes associated with the 1.1 Ga Midcontinent Rift System: *Journal of Geophysical Research*, v. 98.
- PACHT, J.A., 1984, Petrologic evolution and paleogeography of the Late Cretaceous Nanaimo Basin, Washington and British Columbia: implications for Cretaceous tectonics: *Geological Society of America Bulletin*, v. 95, p. 766-778.
- PATRON, C., J.D., W., J.C., H., J.M., H., A., G., AND R., M., 2010, Improved laser ablation U-Pb zircon geochronology through robust downhole fractionation correction: *Geochemistry Geophysics Geosystems*, v. 11, p. 36.
- PETRUS, J.A., AND KAMBER, B.S., 2012, VizualAge: A novel approach to laser ablation ICP-MS U-Pb geochronology data reduction: *Geostandards and Geoanalytical Research*, v. 36, p. 247 - 270.
- PRICE, R.A., AND CARMICHAEL, D.M., 1986, Geometric test for Late Cretaceous-Paleogene intracontinental transform faulting in the Canadian Cordillera: *Geology*, v. 14, p. 468 - 471.
- RAMIREZ, S.G., GULICK, S.P.S., AND HAYMAN, N.W., 2015, Early sedimentation and deformation in the Kumano forearc basin linked with Nankai accretionary prism evolution, southwest Japan: *Geochemistry, Geophysics, Geosystems*, v. 16, p. 1616 - 1633.
- RICHARDSON, J., 1877, Report on the Coalfields of Nanaimo, Comox, Cowichan, Burrard inlet, and Sooke, B.C. Report of Progress: *Geological Survey of Canada*, v. 1876 - 1877, p. 160 - 192.
- RIDGWAY, K.D., TROP, J.M., NIKLEBERG, W.J., DAVIDSON, C.M., AND EASTHAM, K.R., 2002, Mesozoic and Cenozoic tectonics of the eastern and central Alaska Range: Progressive basin development and deformation in a suture zone: *GSA Bulletin*, v. 114, p. 1480 - 1504.

- RUKS, T.W., 2015, Stratigraphy and paleotectonic studies of Paleozoic Wrangellia and its contain volcanogenic massive sulfide (VMS) occurrences, Vancouver Island, British Columbia, Canada: The University of British Columbia, Vancouver, 375 p.
- RUSMORE, M.E., AND WOODSWORTH, G.J., 1991, Coast Plutonic Complex: A mid-Cretaceous contractional orogen: *Geology*, v. 19, p. 941 - 944.
- SAUER, K.B., GORDON, S.M., MILLER, R.B., VERVOOT, J.D., AND FISHER, C.M., 2016, Evolution of the Jura-Cretaceous North American Cordilleran margin: Insights from detrital-zircon U-Pb and Hf isotopes of sedimentary units of the North Cascades Range, Washington: *Geosphere*, v. 13, p. 2094 - 2118.
- SCHERMER, E.R., HOFFNAGLE, E.A., BROWN, E., H., GEHRELS, G.E., AND MCCLELLAND, W.C., 2018, U-Pb and Hf isotopic evidence for an Arctic origin of terranes in northwestern Washington: *Geosphere*, v. 14, p. 835 - 860.
- SICKMANN, Z.T., PAULL, C.K., AND GRAHAM, S.A., 2016, Detrital-zircon mixing and partitioning in fluvial to deep marine systems, Central California, U.S.A.: *Journal of Sedimentary Research*, v. 86, p. 1298 - 1307.
- SLITER, W.V., 1973, Upper Cretaceous foraminifers from the Vancouver Island area, British Columbia, Canada: *Journal of Foraminiferal Research*, v. 3, p. 167 - 186.
- STOMMEL, H., 1957, A survey of ocean current theory: *Deep Sea Research*, v. 4, p. 149 - 184.
- TAKANO, O., 2017, Intermittent Formation, Sedimentation and Deformation History of Cenozoic Forearc Basins along the Northwestern Pacific Margins as an Indicator of Tectonic Scenarios, *in* Itoh, Y., Takano, O., Takashima, R., Nishi, H., and Yoshida, T., eds., *Dynamics of Arc Migration and Amalgamation*, IntechOpen, p. 24.
- TAKANO, O., ITOH, Y., AND KUSUMOTO, S., 2013, Variation in Forearc Basin Configuration and Basin-fillion Depositional Systems as a Function of Trench Slope Break Development and Strike-Slip Movement: Examples from the Cenozoic Ishikari-Sanriku-Oki and Tokai-Oki-Kumano-Nada Forearc Basins, Japan, *in* Itoh, Y., ed., *Mechanism of Sedimentary Basin Formation: Multidisciplinary Approach on Active Plate Margins*, Intech.
- TAKASHIMA, R., KAWABE, F., NISHI, H., MORIYA, K., WANI, R., AND ANDO, H., 2004, Geology and stratigraphy of forearc basin sediments in Hokkaido, Japan: Cretaceous environmental events on the north-west Pacific margin: *Cretaceous Research*, v. 25, p. 365 - 390.
- UMHOEFER, P.J., 1987, Northward translation of the "Baja British Columbia" along the Late Cretaceous to Paleocene margin of western North America: *Tectonics*, v. 6, p. 377 - 394.

- UMHOFER, P.J., AND BLAKEY, R., 2006, Moderate (1600 km) northward translation of Baja British Columbia from southern California: An attempt at reconciliation of paleomagnetism and geology, *in* Haggart, J.W., Enkin, R.J., and Monger, J.W.H., eds., *Paleogeography of the North American Cordillera: Evidence For and Against Large-Scale Displacement: Geological Association of Canada Special Paper*, p. 307 - 329.
- UMHOFER, P.J., AND MILLER, R.B., 1996, Mid-Cretaceous thrusting in the southern Coast Belt, British Columbia and Washington, after strike-slip fault reconstruction: *Tectonics*, v. 15, p. 545 - 565.
- USHER, J.L., 1952, Ammonite faunas of the Upper Cretaceous rocks of Vancouver Island, British Columbia, E. Cloutier, Queen's Printer.
- VAN DER HEYDEN, P., 1992, A Middle Jurassic to Early Tertiary Andean-Sierran arc model for the Coast Belt of British Columbia: *Tectonics*, v. 11, p. 82 - 97.
- VERMEESCH, P., 2004, How many grains are needed for a provenance study?: *Earth and Planetary Science Letters*, v. 224, p. 441 - 451.
- VERMEESCH, P., 2012, On the visualisation of detrital age distributions: *Chemical Geology*, v. 312 - 313, p. 190 - 194.
- VERMEESCH, P., 2013, Multi-sample comparison of detrital age distributions: *Chemical Geology*, v. 341, p. 140 - 146.
- WARD, P.D., 1978, Revisions to the stratigraphy and biochronology of the Upper Cretaceous Nanaimo Group, British Columbia and Washington State: *Canadian Journal of Earth Sciences*, v. 15, p. 405-423.
- WARD, P.D., AND STANLEY, K.O., 1982, The Haslam Formation: A late Santonian-early Campanian forearc basin deposit in the Insular Belt of southwestern British Columbia and adjacent Washington: *Journal of Sedimentary Research*, v. 52, p. 975 - 990.
- WHEELER, J.O., AND MCFEELY, P., 1991, Tectonic Assemblage Map of the Canadian Cordillera and adjacent parts of the United States of America: Geological Survey of Canada.
- WILLIAMS, T.B., 1924, *The Comox Coal Basin*: University of Wisconsin.
- WYLD, S.J., AND UHOFER, P.J., 2006, Reconstructing northern Cordilleran terranes along known Cretaceous and Cenozoic strike-slip faults: Implications for the Baja British Columbia hypothesis and other models: *Geological Association of Canada Special Paper*, v. 46, p. 277 - 298.

YORATH, C.J., GREEN, A.G., CLOWES, R.M., BROWN, A.S., BRANDON, M.T., KANASEWICH, E.R., HYNDMAN, R.D., AND SPENCER, C., 1985, Lithoprobe, southern Vancouver Island: Seismic reflection sees through Wrangellia to the Juan de Fuca plate: *Geology*, v. 13, p. 759 - 762.

Appendix A.

Detrital zircon SEM images

Description:

The accompanying zip file shows scanning electron microscope images of the detrital zircon samples processed at Arizona LaserChron (Samples 7, 16, and 20). A backscatter electron microscopy image is unavailable for sample 20.

Filename:

Appendix A - SEM images.zip

Appendix B.

Detrital zircon mount images

Description:

The accompanying zip file shows visible light images of the detrital zircon mounts processed at Arizona LaserChron (Samples 7, 16, and 20).

Filename:

Appendix B - Mount images.zip

Appendix C.

Detrital zircon supplementary data

Description:

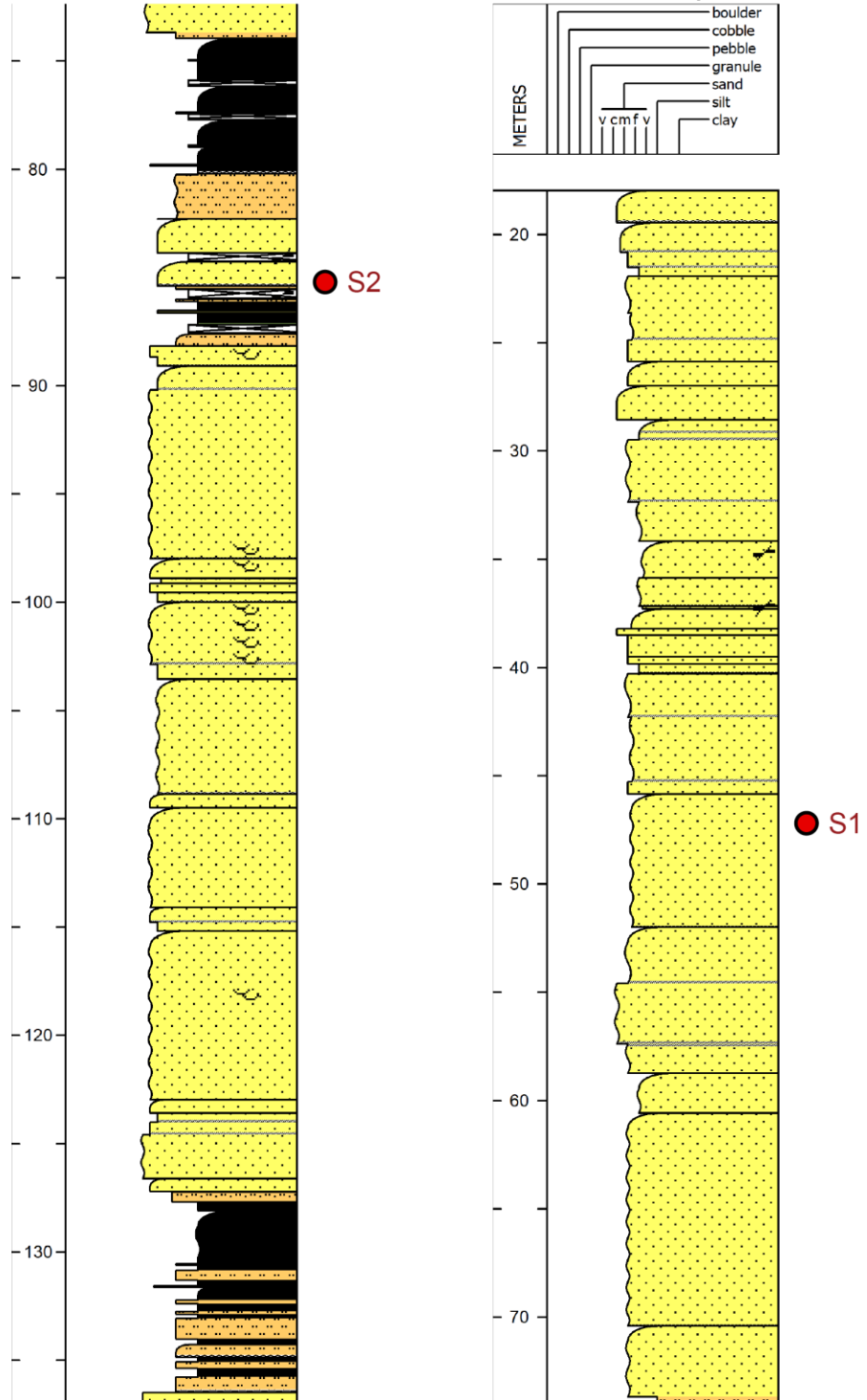
The attached Excel spreadsheet contains coordinates, depositional environment interpretations, alternative maximum depositional age calculations and age data for detrital zircon used in this study.

Filename:

Appendix C - Detrital zircon age data.xlsx

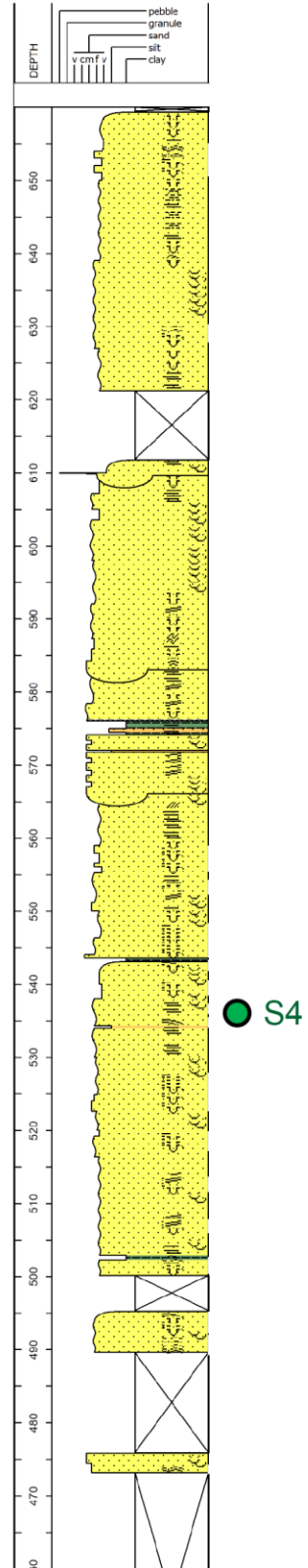
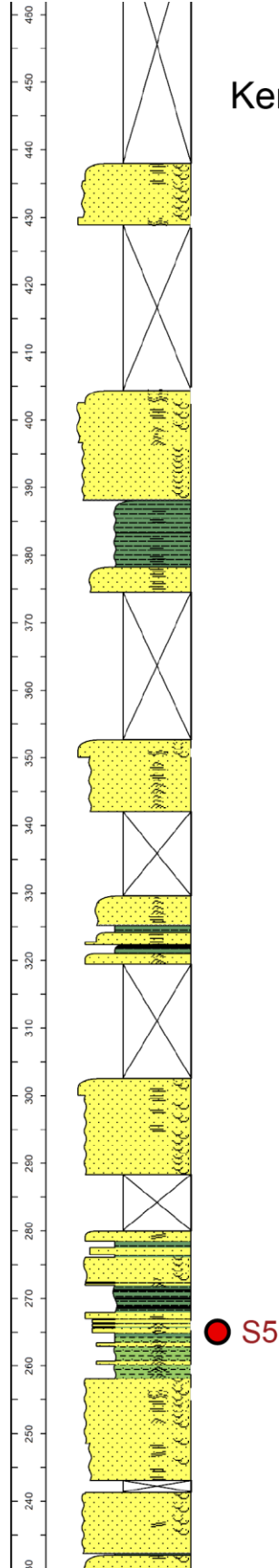
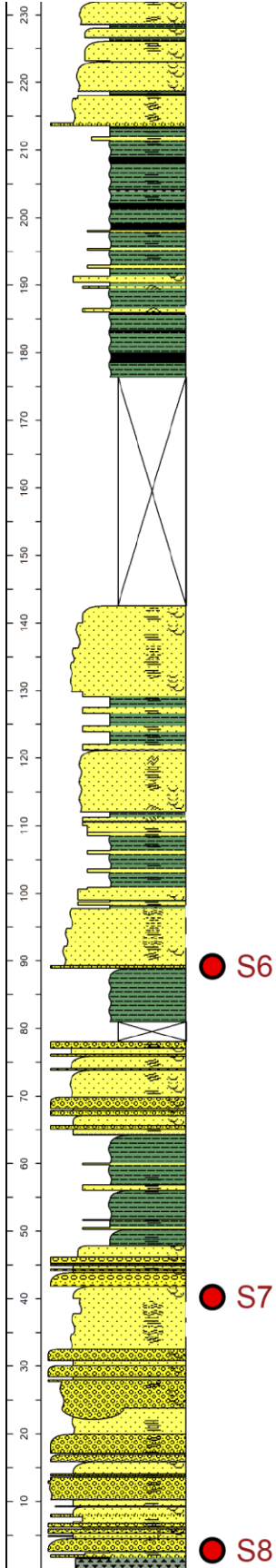
Appendix D. DZ sample positions in core and outcrop

Quinsam Coal Mine Kent et al. in press

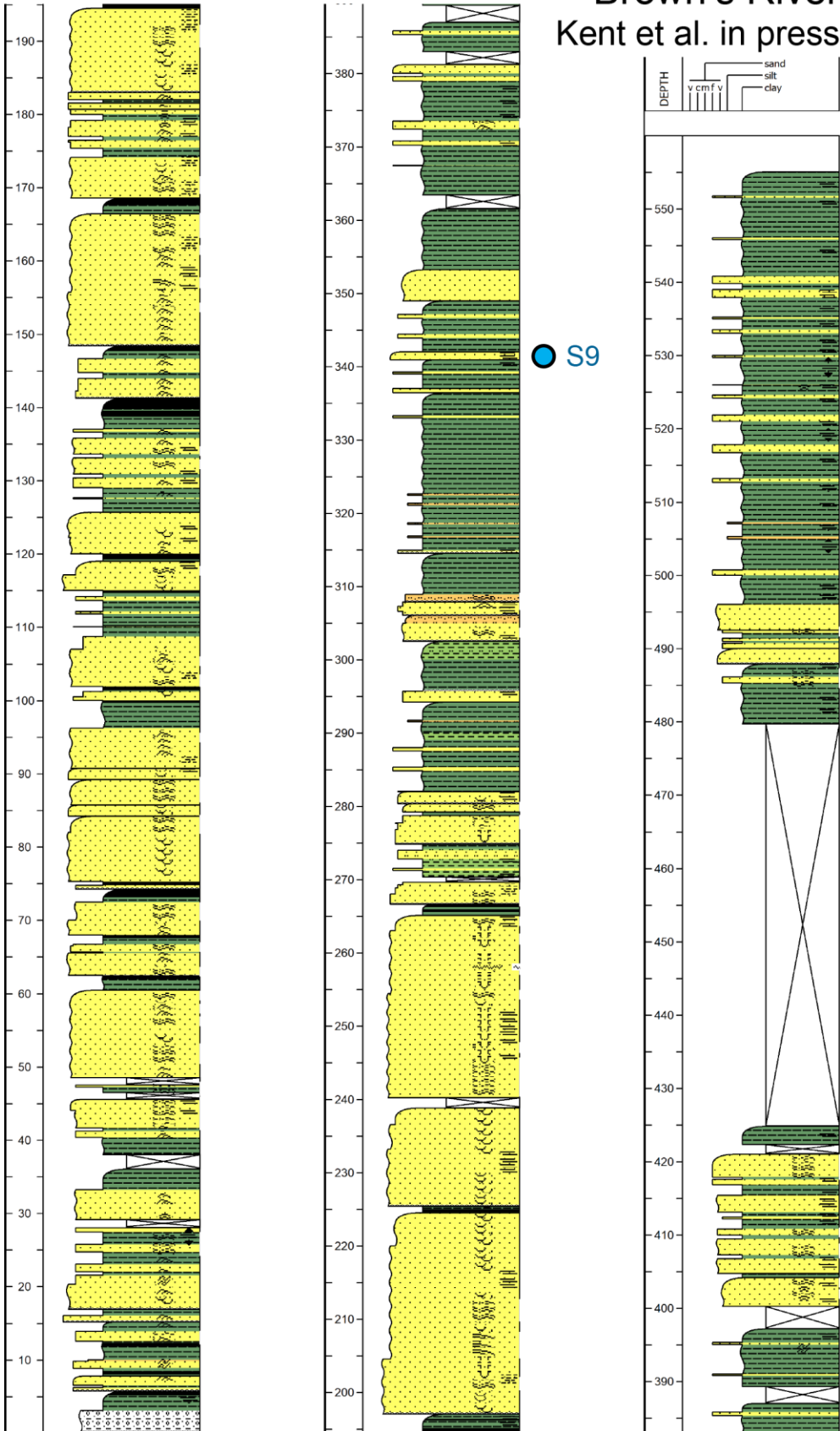


Oyster River

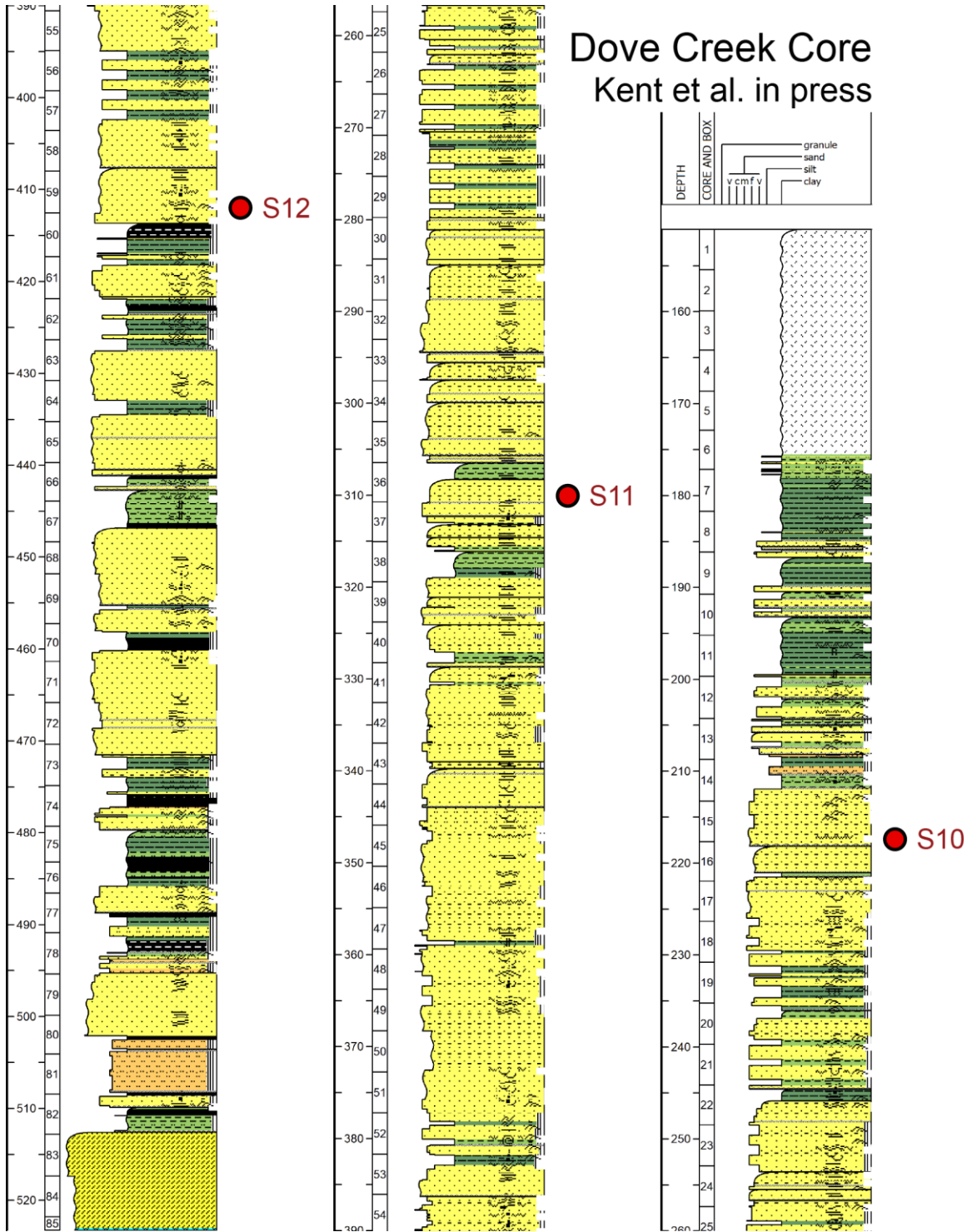
Kent et al. in press



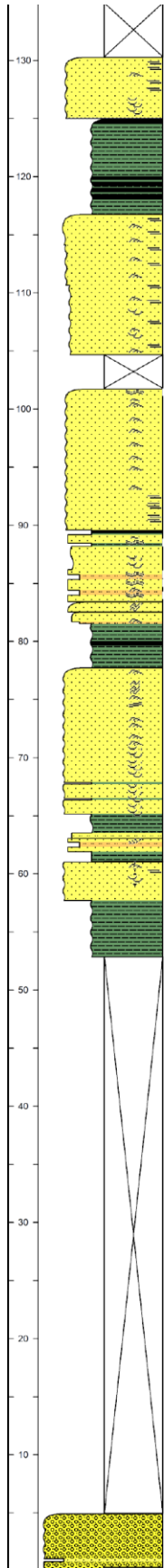
Brown's River Kent et al. in press



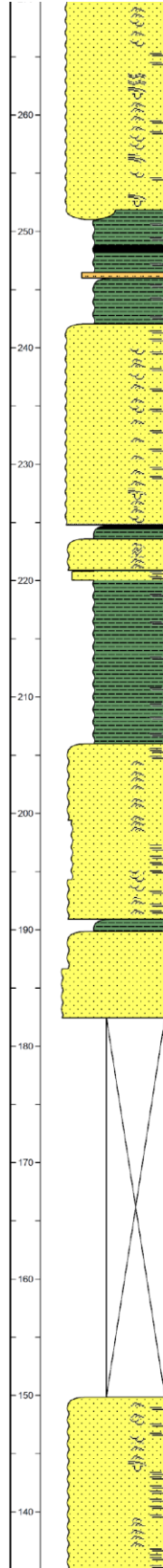
Dove Creek Core Kent et al. in press



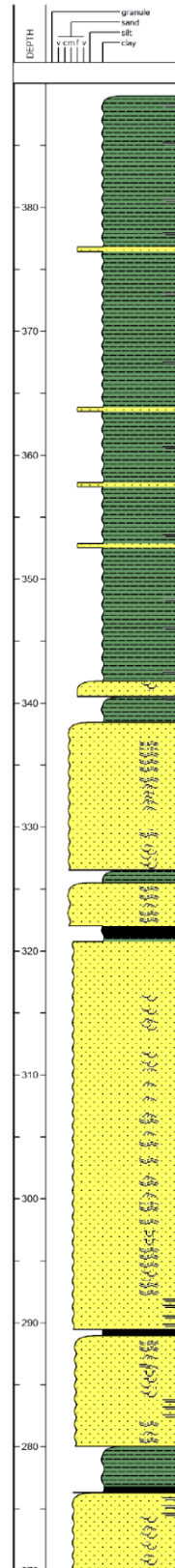
Trent River Kent et al. in press



● S14

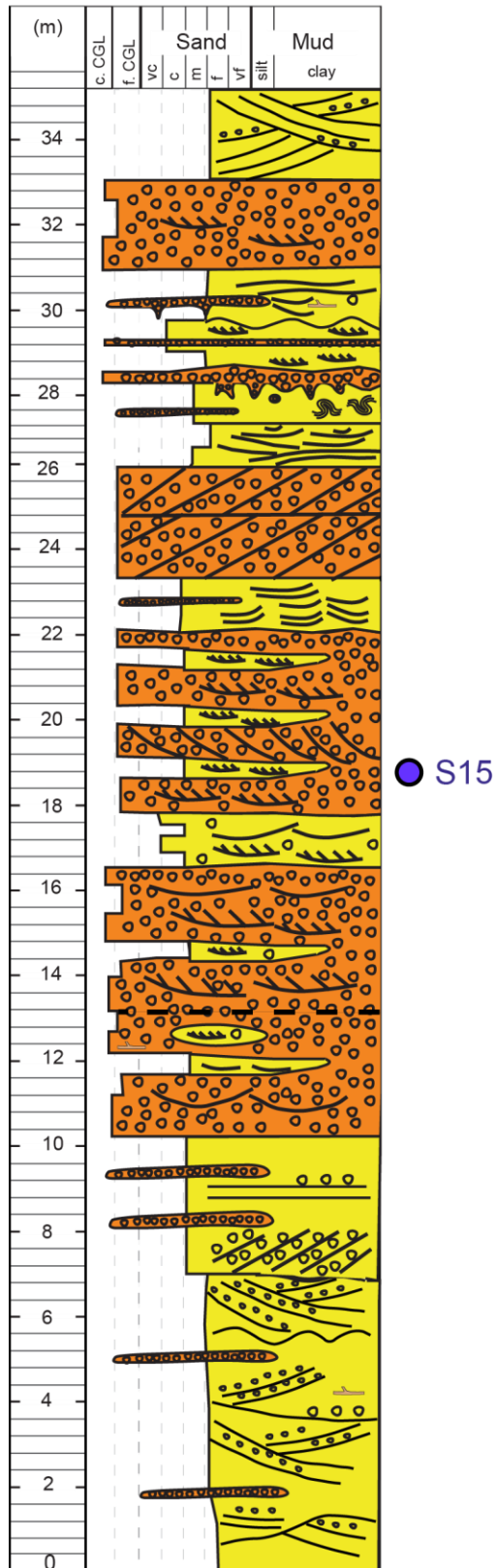


● S13

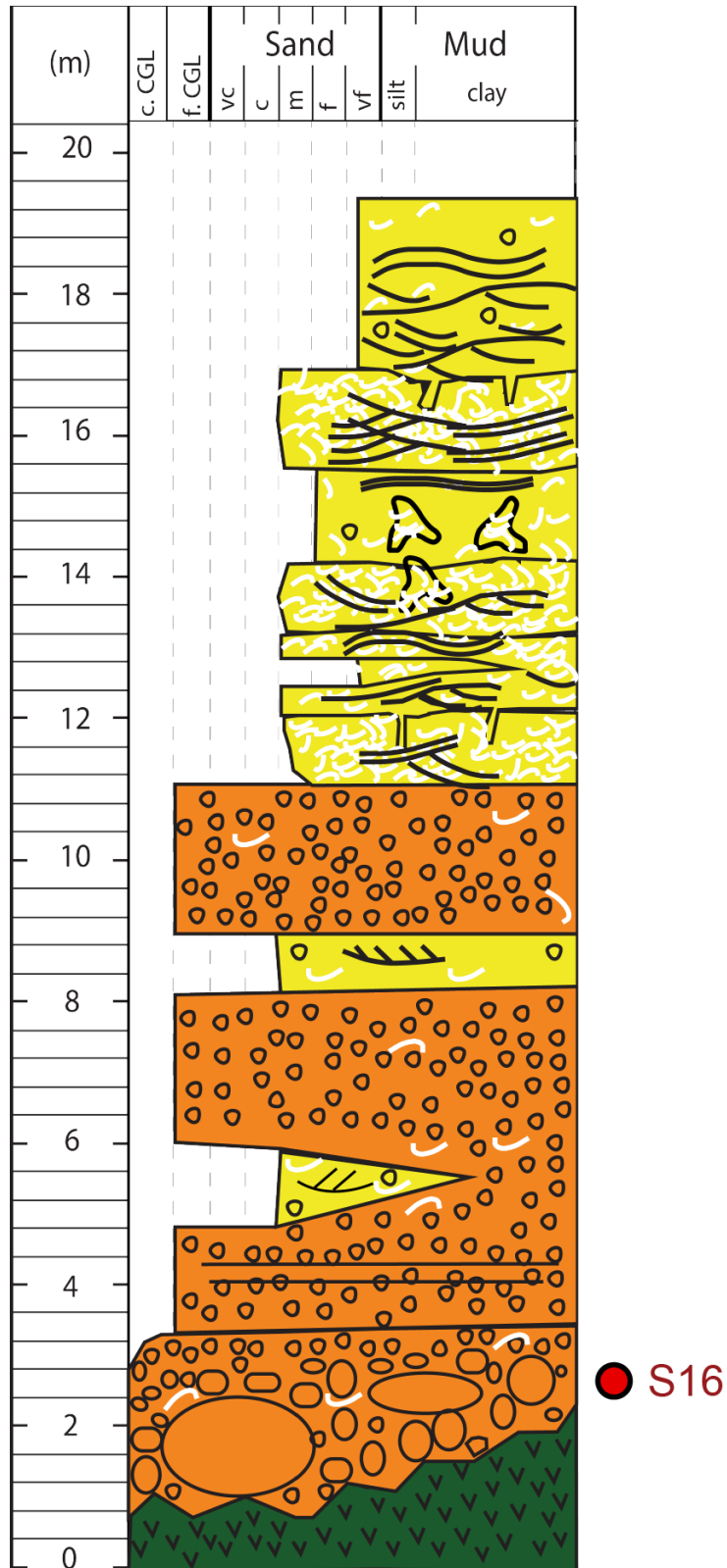


Wall Beach

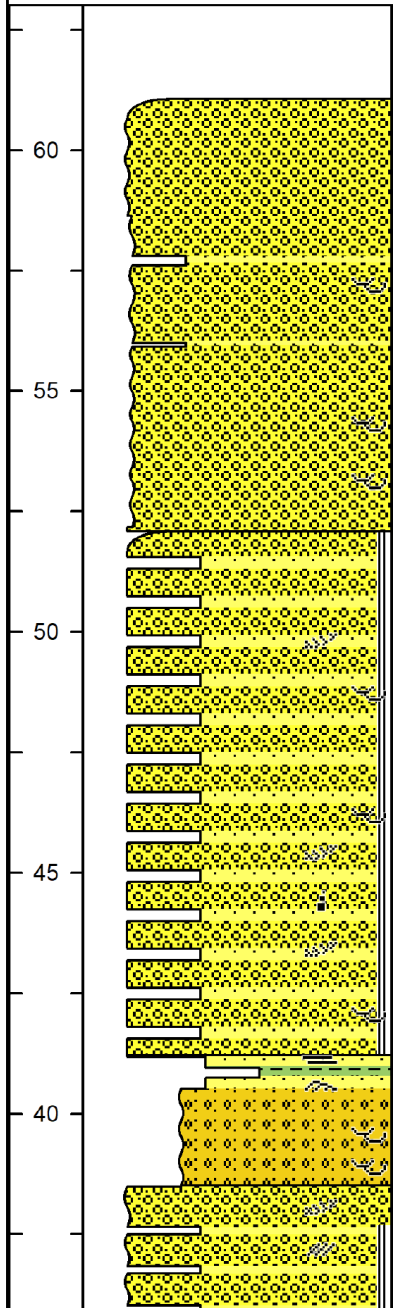
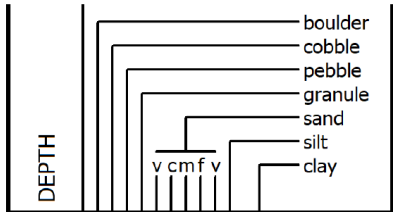
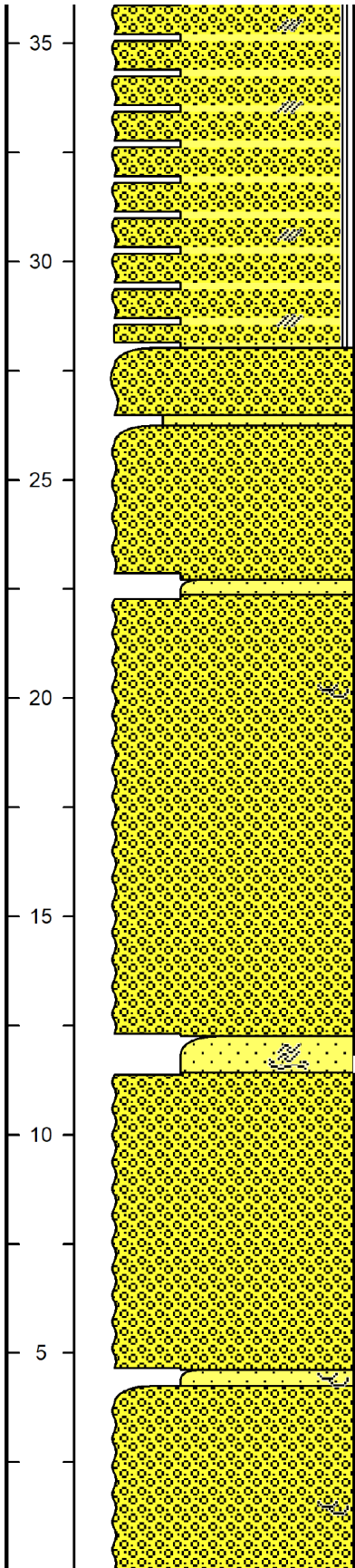
Jones et al. 2018



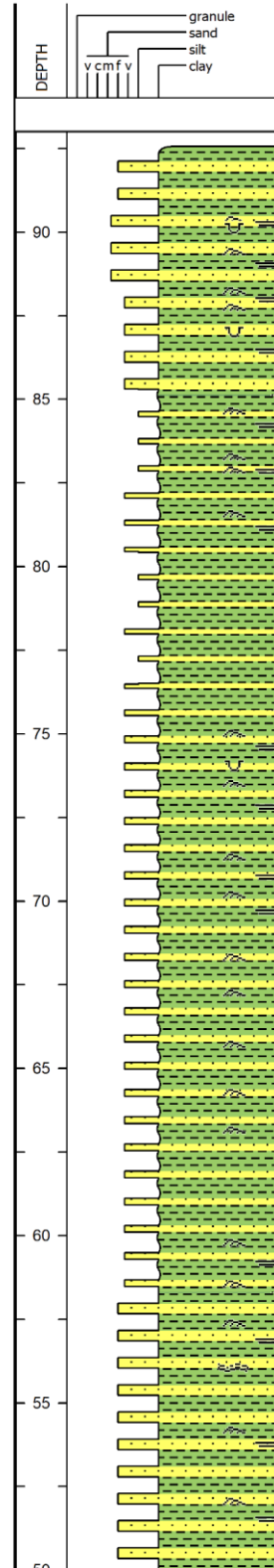
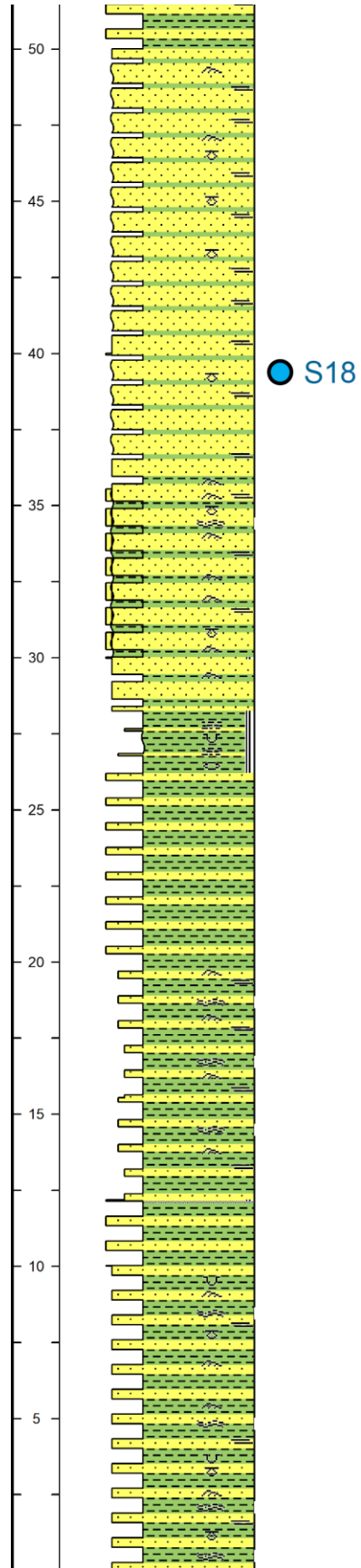
Departure Bay Jones et al. 2018



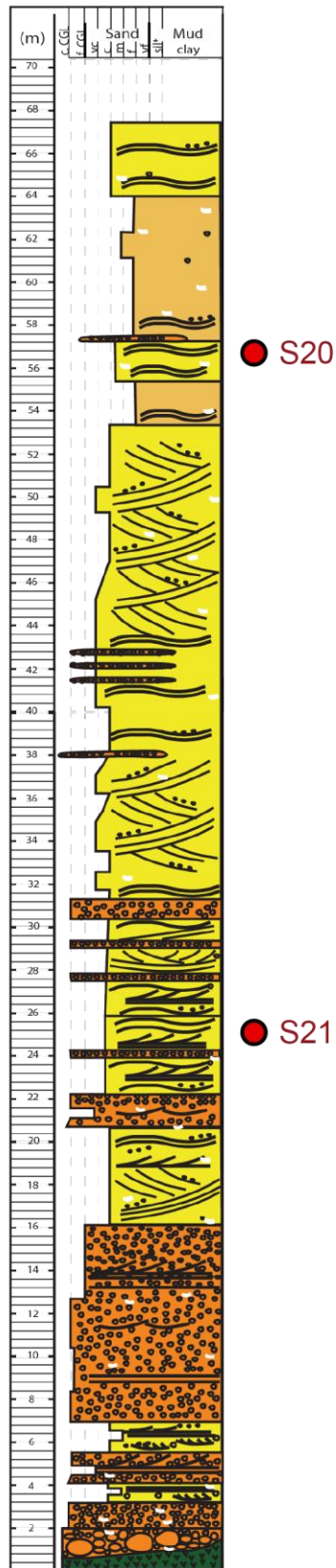
Bare Point Jones 2016



Trestle 66 Jones 2016

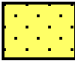








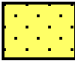








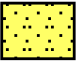
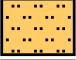






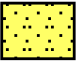
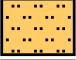






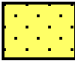








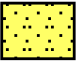
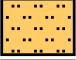








Ruckle Park
Jones et al. 2018

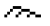


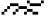



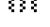







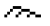


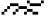



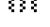







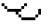

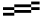
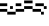
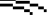




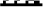
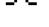




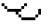

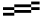
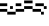
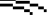




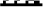
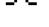




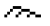


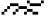



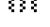







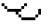

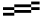
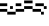
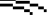




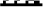
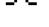






LEGEND

LITHOLOGY

| | | | | | | | | | | | | | | | | | | | | | | | | | | | | | | | | | | | |
|---|---|-----------|---|-----------------|---|-----------------|---|-------|---|----------------|---|---------------|---|----------|---|--------|---|-----------|--|---|-----------------|---|-----------|---|-----------------|---|----------------|---|----------|---|------|---|----------|---|-------------------------------|
| <table border="0" style="width: 100%;"> <tr><td></td><td>Sandstone</td></tr> <tr><td></td><td>Muddy Sandstone</td></tr> <tr><td></td><td>Sandy Siltstone</td></tr> <tr><td></td><td>Shale</td></tr> <tr><td></td><td>Sandy Mudstone</td></tr> <tr><td></td><td>Organic Shale</td></tr> <tr><td></td><td>Paleosol</td></tr> <tr><td></td><td>Basalt</td></tr> <tr><td></td><td>Lost Core</td></tr> </table> |  | Sandstone |  | Muddy Sandstone |  | Sandy Siltstone |  | Shale |  | Sandy Mudstone |  | Organic Shale |  | Paleosol |  | Basalt |  | Lost Core | <table border="0" style="width: 100%;"> <tr><td></td><td>Silty Sandstone</td></tr> <tr><td></td><td>Siltstone</td></tr> <tr><td></td><td>Muddy Siltstone</td></tr> <tr><td></td><td>Silty Mudstone</td></tr> <tr><td></td><td>Mudstone</td></tr> <tr><td></td><td>Coal</td></tr> <tr><td></td><td>Concrete</td></tr> <tr><td></td><td>Volcaniclastic Basalt Breccia</td></tr> </table> |  | Silty Sandstone |  | Siltstone |  | Muddy Siltstone |  | Silty Mudstone |  | Mudstone |  | Coal |  | Concrete |  | Volcaniclastic Basalt Breccia |
|  | Sandstone | | | | | | | | | | | | | | | | | | | | | | | | | | | | | | | | | | |
|  | Muddy Sandstone | | | | | | | | | | | | | | | | | | | | | | | | | | | | | | | | | | |
|  | Sandy Siltstone | | | | | | | | | | | | | | | | | | | | | | | | | | | | | | | | | | |
|  | Shale | | | | | | | | | | | | | | | | | | | | | | | | | | | | | | | | | | |
|  | Sandy Mudstone | | | | | | | | | | | | | | | | | | | | | | | | | | | | | | | | | | |
|  | Organic Shale | | | | | | | | | | | | | | | | | | | | | | | | | | | | | | | | | | |
|  | Paleosol | | | | | | | | | | | | | | | | | | | | | | | | | | | | | | | | | | |
|  | Basalt | | | | | | | | | | | | | | | | | | | | | | | | | | | | | | | | | | |
|  | Lost Core | | | | | | | | | | | | | | | | | | | | | | | | | | | | | | | | | | |
|  | Silty Sandstone | | | | | | | | | | | | | | | | | | | | | | | | | | | | | | | | | | |
|  | Siltstone | | | | | | | | | | | | | | | | | | | | | | | | | | | | | | | | | | |
|  | Muddy Siltstone | | | | | | | | | | | | | | | | | | | | | | | | | | | | | | | | | | |
|  | Silty Mudstone | | | | | | | | | | | | | | | | | | | | | | | | | | | | | | | | | | |
|  | Mudstone | | | | | | | | | | | | | | | | | | | | | | | | | | | | | | | | | | |
|  | Coal | | | | | | | | | | | | | | | | | | | | | | | | | | | | | | | | | | |
|  | Concrete | | | | | | | | | | | | | | | | | | | | | | | | | | | | | | | | | | |
|  | Volcaniclastic Basalt Breccia | | | | | | | | | | | | | | | | | | | | | | | | | | | | | | | | | | |

PHYSICAL STRUCTURES

| | | | | | | | | | | | | | | | | | | | | | | | | | | | | | | | | | | | | | | | | | | | | | | | | | | | | | | | | | | | | | | | | | | | | | | | | | | | | | | | | | | | | | | | | | | | |
|---|---|--------------------------|---------------------|---|---|------------------|---|---|--------------------------|---|---|----------------|---|---|--------------------|---|---|---------|---|---|----------------|---|---|-------------------|---|---|-------------------|---|---|--------------|---|---|--------------------|---|---|-----------|---|---|--------------------|---|---|------------------|---|---|-----------------|--|---|---|---------------------|---|---|----------------------|---|---|----------------------|---|---|---------------|---|---|-----------------------|---|---|-------|---|---|--------------------|---|---|----------------------|---|---|------------|---|---|--------------------|---|---|------------------------|---|---|-----------------|---|---|----------------------|---|---|---------|---|---|-------------|
| <table border="0" style="width: 100%;"> <tr><td></td><td>-</td><td>Current-Ripple Lam.</td></tr> <tr><td></td><td>-</td><td>Sym.-Ripple Lam.</td></tr> <tr><td></td><td>-</td><td>Low-Angle Tab./Tan. Beds</td></tr> <tr><td></td><td>-</td><td>Flaser Bedding</td></tr> <tr><td></td><td>-</td><td>Lenticular Bedding</td></tr> <tr><td></td><td>-</td><td>Churned</td></tr> <tr><td></td><td>-</td><td>Graded Bedding</td></tr> <tr><td></td><td>-</td><td>Synaeresis Cracks</td></tr> <tr><td></td><td>-</td><td>Mud Drapes (Dbl.)</td></tr> <tr><td></td><td>-</td><td>Slickensides</td></tr> <tr><td></td><td>-</td><td>Parallel Bed./Lam.</td></tr> <tr><td></td><td>-</td><td>Slump/SSD</td></tr> <tr><td></td><td>-</td><td>Mud/H. min. drapes</td></tr> <tr><td></td><td>-</td><td>Climbing Ripples</td></tr> <tr><td></td><td>-</td><td>-Horiz. Slicks.</td></tr> </table> |  | - | Current-Ripple Lam. |  | - | Sym.-Ripple Lam. |  | - | Low-Angle Tab./Tan. Beds |  | - | Flaser Bedding |  | - | Lenticular Bedding |  | - | Churned |  | - | Graded Bedding |  | - | Synaeresis Cracks |  | - | Mud Drapes (Dbl.) |  | - | Slickensides |  | - | Parallel Bed./Lam. |  | - | Slump/SSD |  | - | Mud/H. min. drapes |  | - | Climbing Ripples |  | - | -Horiz. Slicks. | <table border="0" style="width: 100%;"> <tr><td></td><td>-</td><td>Trough Cross-strat.</td></tr> <tr><td></td><td>-</td><td>Climbing-Ripple Lam.</td></tr> <tr><td></td><td>-</td><td>Gently Inclined Lam.</td></tr> <tr><td></td><td>-</td><td>Wavy Bed./Lam</td></tr> <tr><td></td><td>-</td><td>Hummocky Cross-strat.</td></tr> <tr><td></td><td>-</td><td>Scour</td></tr> <tr><td></td><td>-</td><td>Micro-fault (sed.)</td></tr> <tr><td></td><td>-</td><td>Reactivation Surface</td></tr> <tr><td></td><td>-</td><td>Load Casts</td></tr> <tr><td></td><td>-</td><td>Lenticular Bedding</td></tr> <tr><td></td><td>-</td><td>Fluid-Esc. Str./Dishes</td></tr> <tr><td></td><td>-</td><td>Bipolar Ripples</td></tr> <tr><td></td><td>-</td><td>Combined Flow Ripple</td></tr> <tr><td></td><td>-</td><td>-Rubble</td></tr> <tr><td></td><td>-</td><td>Gutter Cast</td></tr> </table> |  | - | Trough Cross-strat. |  | - | Climbing-Ripple Lam. |  | - | Gently Inclined Lam. |  | - | Wavy Bed./Lam |  | - | Hummocky Cross-strat. |  | - | Scour |  | - | Micro-fault (sed.) |  | - | Reactivation Surface |  | - | Load Casts |  | - | Lenticular Bedding |  | - | Fluid-Esc. Str./Dishes |  | - | Bipolar Ripples |  | - | Combined Flow Ripple |  | - | -Rubble |  | - | Gutter Cast |
|  | - | Current-Ripple Lam. | | | | | | | | | | | | | | | | | | | | | | | | | | | | | | | | | | | | | | | | | | | | | | | | | | | | | | | | | | | | | | | | | | | | | | | | | | | | | | | | | | | | | | | | | |
|  | - | Sym.-Ripple Lam. | | | | | | | | | | | | | | | | | | | | | | | | | | | | | | | | | | | | | | | | | | | | | | | | | | | | | | | | | | | | | | | | | | | | | | | | | | | | | | | | | | | | | | | | | |
|  | - | Low-Angle Tab./Tan. Beds | | | | | | | | | | | | | | | | | | | | | | | | | | | | | | | | | | | | | | | | | | | | | | | | | | | | | | | | | | | | | | | | | | | | | | | | | | | | | | | | | | | | | | | | | |
|  | - | Flaser Bedding | | | | | | | | | | | | | | | | | | | | | | | | | | | | | | | | | | | | | | | | | | | | | | | | | | | | | | | | | | | | | | | | | | | | | | | | | | | | | | | | | | | | | | | | | |
|  | - | Lenticular Bedding | | | | | | | | | | | | | | | | | | | | | | | | | | | | | | | | | | | | | | | | | | | | | | | | | | | | | | | | | | | | | | | | | | | | | | | | | | | | | | | | | | | | | | | | | |
|  | - | Churned | | | | | | | | | | | | | | | | | | | | | | | | | | | | | | | | | | | | | | | | | | | | | | | | | | | | | | | | | | | | | | | | | | | | | | | | | | | | | | | | | | | | | | | | | |
|  | - | Graded Bedding | | | | | | | | | | | | | | | | | | | | | | | | | | | | | | | | | | | | | | | | | | | | | | | | | | | | | | | | | | | | | | | | | | | | | | | | | | | | | | | | | | | | | | | | | |
|  | - | Synaeresis Cracks | | | | | | | | | | | | | | | | | | | | | | | | | | | | | | | | | | | | | | | | | | | | | | | | | | | | | | | | | | | | | | | | | | | | | | | | | | | | | | | | | | | | | | | | | |
|  | - | Mud Drapes (Dbl.) | | | | | | | | | | | | | | | | | | | | | | | | | | | | | | | | | | | | | | | | | | | | | | | | | | | | | | | | | | | | | | | | | | | | | | | | | | | | | | | | | | | | | | | | | |
|  | - | Slickensides | | | | | | | | | | | | | | | | | | | | | | | | | | | | | | | | | | | | | | | | | | | | | | | | | | | | | | | | | | | | | | | | | | | | | | | | | | | | | | | | | | | | | | | | | |
|  | - | Parallel Bed./Lam. | | | | | | | | | | | | | | | | | | | | | | | | | | | | | | | | | | | | | | | | | | | | | | | | | | | | | | | | | | | | | | | | | | | | | | | | | | | | | | | | | | | | | | | | | |
|  | - | Slump/SSD | | | | | | | | | | | | | | | | | | | | | | | | | | | | | | | | | | | | | | | | | | | | | | | | | | | | | | | | | | | | | | | | | | | | | | | | | | | | | | | | | | | | | | | | | |
|  | - | Mud/H. min. drapes | | | | | | | | | | | | | | | | | | | | | | | | | | | | | | | | | | | | | | | | | | | | | | | | | | | | | | | | | | | | | | | | | | | | | | | | | | | | | | | | | | | | | | | | | |
|  | - | Climbing Ripples | | | | | | | | | | | | | | | | | | | | | | | | | | | | | | | | | | | | | | | | | | | | | | | | | | | | | | | | | | | | | | | | | | | | | | | | | | | | | | | | | | | | | | | | | |
|  | - | -Horiz. Slicks. | | | | | | | | | | | | | | | | | | | | | | | | | | | | | | | | | | | | | | | | | | | | | | | | | | | | | | | | | | | | | | | | | | | | | | | | | | | | | | | | | | | | | | | | | |
|  | - | Trough Cross-strat. | | | | | | | | | | | | | | | | | | | | | | | | | | | | | | | | | | | | | | | | | | | | | | | | | | | | | | | | | | | | | | | | | | | | | | | | | | | | | | | | | | | | | | | | | |
|  | - | Climbing-Ripple Lam. | | | | | | | | | | | | | | | | | | | | | | | | | | | | | | | | | | | | | | | | | | | | | | | | | | | | | | | | | | | | | | | | | | | | | | | | | | | | | | | | | | | | | | | | | |
|  | - | Gently Inclined Lam. | | | | | | | | | | | | | | | | | | | | | | | | | | | | | | | | | | | | | | | | | | | | | | | | | | | | | | | | | | | | | | | | | | | | | | | | | | | | | | | | | | | | | | | | | |
|  | - | Wavy Bed./Lam | | | | | | | | | | | | | | | | | | | | | | | | | | | | | | | | | | | | | | | | | | | | | | | | | | | | | | | | | | | | | | | | | | | | | | | | | | | | | | | | | | | | | | | | | |
|  | - | Hummocky Cross-strat. | | | | | | | | | | | | | | | | | | | | | | | | | | | | | | | | | | | | | | | | | | | | | | | | | | | | | | | | | | | | | | | | | | | | | | | | | | | | | | | | | | | | | | | | | |
|  | - | Scour | | | | | | | | | | | | | | | | | | | | | | | | | | | | | | | | | | | | | | | | | | | | | | | | | | | | | | | | | | | | | | | | | | | | | | | | | | | | | | | | | | | | | | | | | |
|  | - | Micro-fault (sed.) | | | | | | | | | | | | | | | | | | | | | | | | | | | | | | | | | | | | | | | | | | | | | | | | | | | | | | | | | | | | | | | | | | | | | | | | | | | | | | | | | | | | | | | | | |
|  | - | Reactivation Surface | | | | | | | | | | | | | | | | | | | | | | | | | | | | | | | | | | | | | | | | | | | | | | | | | | | | | | | | | | | | | | | | | | | | | | | | | | | | | | | | | | | | | | | | | |
|  | - | Load Casts | | | | | | | | | | | | | | | | | | | | | | | | | | | | | | | | | | | | | | | | | | | | | | | | | | | | | | | | | | | | | | | | | | | | | | | | | | | | | | | | | | | | | | | | | |
|  | - | Lenticular Bedding | | | | | | | | | | | | | | | | | | | | | | | | | | | | | | | | | | | | | | | | | | | | | | | | | | | | | | | | | | | | | | | | | | | | | | | | | | | | | | | | | | | | | | | | | |
|  | - | Fluid-Esc. Str./Dishes | | | | | | | | | | | | | | | | | | | | | | | | | | | | | | | | | | | | | | | | | | | | | | | | | | | | | | | | | | | | | | | | | | | | | | | | | | | | | | | | | | | | | | | | | |
|  | - | Bipolar Ripples | | | | | | | | | | | | | | | | | | | | | | | | | | | | | | | | | | | | | | | | | | | | | | | | | | | | | | | | | | | | | | | | | | | | | | | | | | | | | | | | | | | | | | | | | |
|  | - | Combined Flow Ripple | | | | | | | | | | | | | | | | | | | | | | | | | | | | | | | | | | | | | | | | | | | | | | | | | | | | | | | | | | | | | | | | | | | | | | | | | | | | | | | | | | | | | | | | | |
|  | - | -Rubble | | | | | | | | | | | | | | | | | | | | | | | | | | | | | | | | | | | | | | | | | | | | | | | | | | | | | | | | | | | | | | | | | | | | | | | | | | | | | | | | | | | | | | | | | |
|  | - | Gutter Cast | | | | | | | | | | | | | | | | | | | | | | | | | | | | | | | | | | | | | | | | | | | | | | | | | | | | | | | | | | | | | | | | | | | | | | | | | | | | | | | | | | | | | | | | | |